Effect of Coolant Temperature on Performance and Emissions of a Compression Ignition Engine Running on Conventional Diesel and Hydrotreated Vegetable Oil (HVO)

energies

MDPI

Article

Effect of Coolant Temperature on Performance and Emissions of a Compression Ignition Engine Running on Conventional Diesel and Hydrotreated Vegetable Oil (HVO)

Alessandro Mancarella and Omar Marello *

Energy Department, Politecnico di Torino, Corso Duca degli Abruzzi 24, 10129 Torino, Italy
* Correspondence: omar.marello@polito.it

Abstract: To meet future goals of energy sustainability and carbon neutrality, disruptive changes to the current energy mix will be required, and it is expected that renewable fuels, such as hydrotreated vegetable oil (HVO), will play a significant role. To determine how these fuels can transition from pilot scale to the commercial marketplace, extensive research remains needed within the transportation sector. It is well-known that cold engine thermal states, which represent an inevitable portion of a vehicle journey, have significant drawbacks, such as increased incomplete combustion emissions and higher fuel consumption. In view of a more widespread HVO utilization, it is crucial to evaluate its performance under these conditions. In the literature, detailed studies upon these topics are rarely found, especially when HVO is dealt with. Consequently, the aim of this study is to investigate performance and exhaust pollutant emissions of a compression ignition engine running on either regular (petroleum-derived) diesel or HVO at different engine thermal states. This study shows the outcomes of warm-up/cool-down ramps (from cold starts), carried out on two engine operating points (low and high loads) without modifying the original baseline diesel-oriented calibration. Results of calibration parameter sweeps are also shown (on the same engine operating points), with the engine maintained at either high or low coolant temperature while combustion phasing, fuel injection pressure, and intake air flow rate are varied one-factor at a time, to highlight their individual effect on exhaust emissions and engine performance. HVO proved to produce less engine-out incomplete combustion species and soot under all examined conditions and to exhibit greater tolerance of calibration parameter changes compared to diesel, with benefits over conventional fuel intensifying at low coolant temperatures. This would potentially make room for engine recalibration to exploit higher exhaust gas recirculation, delayed injection timings, and/or lower fuel injection pressures to further optimize nitrogen oxides/thermal efficiency trade-off.

Keywords: pollutant emissions; diesel engine; HVO; drop-in fuel; coolant temperature; cold start; ECU calibration

Citation: Mancarella, A.; Marello, O. Effect of Coolant Temperature on Performance and Emissions of a Compression Ignition Engine Running on Conventional Diesel and Hydrotreated Vegetable Oil (HVO). *Energies* **2023**, *16*, 144. https://doi.org/10.3390/en16010144

Academic Editor: Dimitrios C. Rakopoulos

Received: 30 November 2022
Revised: 15 December 2022
Accepted: 16 December 2022
Published: 23 December 2022

1. Introduction

Climate change caused by anthropogenic emissions of greenhouse gases (GHG) from fossil fuels is one of the major global challenges and requires urgent implementation of effective political, social, and technological solutions in the short, medium, and long term. The transport sector already plays a decisive role in this challenge. At the European level, transport accounts for more than a quarter of GHG emissions [1], mainly because the internal combustion engine (ICE) powered by fossil fuels still remains its main source of energy [2]. The global warming potential (GWP) of ICEs is mainly driven by the direct use of petroleum-derived fuels and their conversion to CO_2 during combustion, although emissions of CH_4 and N_2O may have even greater GWP than CO_2. However, while CH_4 and N_2O emissions can be curbed by proper after-treatment system (ATS) technology, the only approach to reduce anthropogenic CO_2 emissions from ICEs is to limit fossil fuel consumption [3]. This can be done by further improving engine thermal efficiency and/or

using biofuels that rely on renewable feedstocks that absorb CO_2 from the atmosphere when produced [4].

The EU has been attempting to promote the use of biofuels to reduce GHG emissions for the past decade. Biofuels can diversify the fuel source for the transport industry, hence enhancing energy independence and diversifying manufacturing sites. In addition, many of these biofuels are compatible with existing propulsion systems and fuel infrastructure [5]. GHG emissions are certainly a primary legislative driver, but it is also important to consider other environmental impacts as well, such as air pollution [6], which poses major health risks to human beings [7].

As far as compression ignition (CI) engines are concerned, diesel combustion tends to produce high nitrogen oxides (NO_x) and particulate matter (PM). The formation of nitrogen oxides follows primarily the so-called "thermal mechanism" [8,9], which is highly dependent on local in-cylinder temperatures and oxygen concentrations. PM emissions are governed by the balance of competing soot production and soot oxidation processes [10]. The former is determined by the availability of acetylene, the formation of polycyclic aromatic hydrocarbons (PAHs) and the inception of soot particles, all of which are processes that are highly dependent on in-cylinder temperatures and air-fuel mixing. The latter is determined by the availability of hydroxyl radicals, oxygen, and temperature as well [11]. All of these mechanisms are difficult to curb; therefore, exhaust pollutant emission targets are still difficult to meet for CI engines, despite that continuous efforts have been made to optimize in-cylinder combustion [12], engine components [13], ATS [14], and to develop combustion control techniques [15–19].

Biomass-derived diesel-like fuels offer a viable solution to all these problems, as they reduce both air pollution and the GHG impact of CI engines. Vegetable oils, animal fats, and waste cooking oils are some of the renewable feedstocks that can be used to make diesel substitutes via various production methods. However, the resulting fuels may have diverse chemical compositions and characteristics [20,21].

First-generation biodiesel, commonly known as biodiesel, is mainly composed of fatty acid methyl esters (FAME) [22]. It is produced, via a transesterification process, from oil-rich crops such as soybean or rapeseed. FAME provides various advantages over petroleum-derived diesel, including improved ignition and lower pollutant emissions, primarily CO, unburned hydrocarbons (HC), and PM [23]. Its application, however, is restricted due to a number of inconveniences, such as its decreased oxidation stability and unfavorable cold flow properties [24]. Indeed, FAME can cause ageing of polymeric materials commonly used in vehicle fuel systems and corrosion of fuel storage tanks [25]. In addition, at low temperatures, FAME tends to create waxy crystals, making its storage problematic, and to degrade cold engine operation because of its higher viscosity [26]. Due to these unfavorable properties, restrictions are generally imposed on the blending of FAME with conventional petroleum-derived diesel (e.g., for the European standard EN 590, in all EU member states, the maximum FAME concentration is set at 7%-vol) [27]. Nevertheless, an interesting upside of FAME is its high lubricity, which is beneficial for components in the injection system that require lubrication from the fuel [28].

Hydrotreated vegetable oil (HVO) could be a viable alternative to FAME. It is a synthetic liquid biofuel whose chemical composition consists of straight-chain paraffinic hydrocarbons (i.e., C_nH_{2n+2} alkanes), free of aromatic compounds, oxygen, and sulfur. It is derived from hydrotreating catalysis of triglyceride-based biomass [29] such as vegetable oils, animal fats, and waste products [30]. Hydrotreatment has a number of upsides over transesterification, including lower processing costs, greater flexibility of raw materials, and greater compatibility with conventional ICEs and fuel standards [31,32]: HVO may be utilized in any proportion in this regard, i.e., either pure or combined with petroleum-based diesel, with little to no adjustments to existing CI engines [33]. Relatively high cetane number and heating value, lower viscosity, and cloud point as well as better cold flow properties [34,35] are some of the benefits HVO can bring over FAME, as thoroughly explored in the literature [33]. In addition, HVO generally features a shorter ignition delay

(ID) and, as a consequence, a more advanced start of combustion (SOC), compared to conventional diesel [36], with a direct impact on engine performance and exhaust pollutant emissions [37,38].

Most of the available literature agrees that HVO reduces the emission of incomplete combustion species (CO and HC) when compared to regular diesel [26,27,29,30,33,39,40], due to higher cetane number and better ignition [26,39]. This might be particularly beneficial at low loads and/or when the engine has not yet warmed up, since incomplete combustion is likely to occur near relatively colder surfaces of the combustion chamber and the tailpipe emission of these chemical species cannot be cut down by the after-treatment system upon cold start, due to poor conversion efficiencies. Proper management and optimization of the engine behavior during warm-up is, therefore, of paramount importance [41], especially considering that a significant part of the car journeys is done after the vehicle has been parked for at least 3 to 8 h and may, thus, include a cold start as an unavoidable part of the daily driving [42]. However, in the published literature, there is only a small number of in-depth research studies on the interactions between engine thermal level and the combustion process, including an examination of the combined impacts of coolant temperature and the most important engine calibration parameters, such as exhaust gas recirculation (EGR) rate, injection time, rail pressure. Furthermore, there is even less research about this topic using HVO. Therefore, this research has the goal of examining exhaust emissions and engine performance of an engine operating on either HVO or conventional diesel, with a focus on the distinct impact of low and high coolant temperatures when using these two fuels, with a remark on how emissions and performance of an engine change between a cold start and a test bench condition where the engine is cooled down by keeping the coolant water temperature "artificially" low.

2. Materials and Methods

2.1. Engine and Experimental Setup

An experimental test campaign was carried out on a fully instrumented 2.3-L four-stroke prototype diesel engine. This engine, whose basic production version is used for modern light-duty commercial vehicles, was installed on a dynamic test bench at Politecnico di Torino's ICE Advanced Laboratory, equipped with an ELIN AVL APA100 cradle-mounted AC dynamometer with nominal torque and power ratings of 525 Nm and 220 kW, respectively. The main technical specifications of the tested engine are reported below, in Table 1.

Table 1. Main technical specifications of the tested CI engine.

Number of cylinders	4
Displacement	2.3 L
Compression ratio	~16:1
Valves per cylinder	4
Turbocharger	Single-stage VGT
Fuel injection system	Common-rail injection system
EGR circuit type	Dual-loop, water-cooled

The aforementioned engine has a high-pressure common-rail injection system with solenoid injectors. On the air/EGR side, the engine is equipped with a variable geometry turbine (VGT), an intake throttle valve, an exhaust flap, and a dual-loop cooled EGR system, which consists of both a high-pressure (HP) and low-pressure (LP) EGR circuit. The baseline (diesel-oriented) calibration of the tested engine uses only the high-pressure EGR circuit.

The ATS installed on the test bench consists of a diesel oxidation catalyst (DOC) and a diesel particulate filter (DPF). A selective catalytic reduction (SCR) system, which is present in commercial applications of this engine, was not available in the current configuration. During the experimental campaign, periodic passive regeneration of the DPF was necessary to prevent the system from clogging.

Suitable sensors (e.g., pressure transducers, thermocouples, volumetric flowmeters, etc.) were fitted at various points throughout the engine circuit in order to make low-frequency measurements. Furthermore, high-frequency Kistler 6058A piezoelectric transducers were employed to measure, every 0.1 crank angle degree (°CA), the pressure inside each of the four cylinders of the engine. In addition, an absolute pressure sensor, a Kistler 4007C piezoresistive transducer, was fitted in the intake manifold to reference the four in-cylinder pressure signals.

As depicted in Figure 1, fuel flow measurement is handled by an AVL KMA 4000 system, which allows continuous measurements of engine fuel consumption with an accuracy of 0.1%, while an AVL AMAi60 exhaust gas analyzer was used to measure NO_x/NO, HC, CO, CO_2, and O_2 volumetric concentrations upstream and downstream of the ATS, as well as CO_2 concentrations in the intake manifold (in order to estimate the EGR rate). Soot emissions were measured, under steady-state conditions, using an AVL 415S smoke-meter.

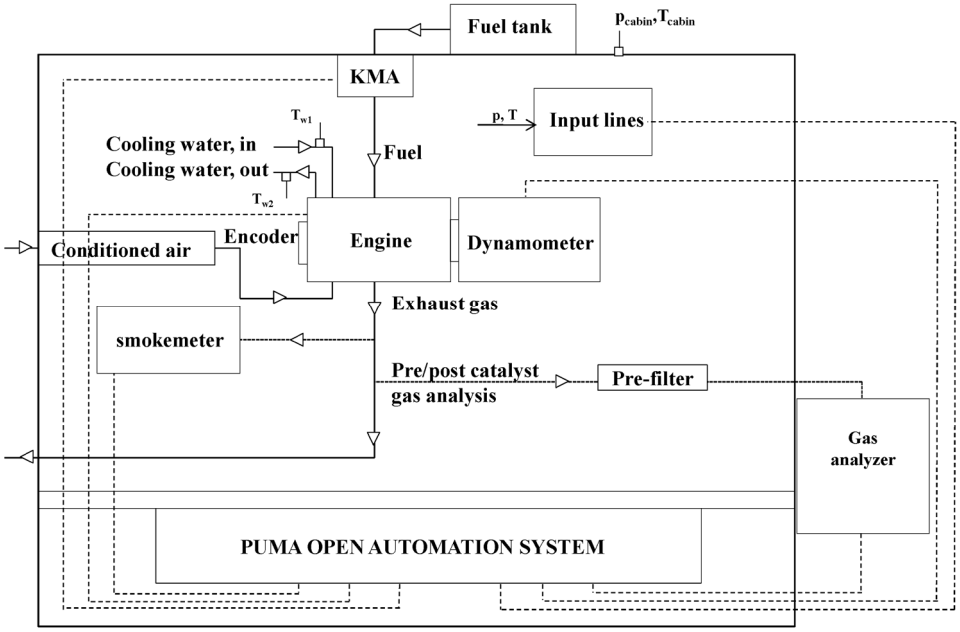

Figure 1. Schematics of the engine test bench.

All of the aforesaid measurement equipment was managed by AVL PUMA Open 2 software, while IndiCom and AVL CONCERTO 5 were used for indicating measurements and data postprocessing, respectively. ETAS INCA was also used for real-time monitoring, calibration, and recording of data through the ETK (German acronym for emulator test probe) interface of the engine electronic control unit (ECU).

Tables 2 and 3 report the available data to establish the accuracy of the measured pollutant emission values. Previous works [43] have shown that the expanded uncertainties of pollutant emission measurements taken at this engine test facility fall within a 2–4% range. As far as the extended uncertainties pertaining to the brake specific emissions are concerned, the fuel flow rate system accuracy (0.1% over a 0.28–110 kg/h fuel flow rate measurement range) and the maximum errors of the engine speed (1.50 rpm at full scale) and torque (0.30 Nm at full scale) also have to be considered [13].

2.2. Tested Fuels

The fuels employed in the experimental campaign presented in this research were conventional diesel B7, derived from petroleum (with up to 7% biodiesel, in compliance with EN 590 standard) and HVO. The main properties of both fuels are listed in Table 4.

This table includes information such as density at 15 °C (lower for HVO), cetane number (higher for HVO owing to its paraffinic nature), and average chemical composition.

Table 2. Composition of the gas calibration cylinders and extended uncertainty (95% confidence interval).

Composition of the Gas Calibration Cylinder and Extended Uncertainty	
NO (lower range) [ppm]	89.7 ± 1.7
NO (higher range) [ppm]	919 ± 18
CO (lower range) [ppm]	4030 ± 79
CO (higher range) [%]	8.370 ± 0.097
CO_2 (lower range) [ppm]	4.980 ± 0.067
CO_2 (higher range) [%]	16.78 ± 0.15
C_3H_8 (lower range) [ppm]	88.8 ± 1.8
C_3H_8 (higher range) [ppm]	1820 ± 36

Table 3. Manufacturer's data for the measurement errors of emission analyzers.

Measurement Errors of Emission Analyzers	
Linearity	≤1% of full-scale range ≤2% of measured value whichever is smaller
Drift 24 h	≤1% of full-scale range
Reproducibility	≤0.5% of full-scale range

Table 4. Diesel vs. HVO main properties.

Parameter	Unit	EN590 Diesel	HVO
Density at 15 °C	kg/m^3	830.6	777.8
Kinematic viscosity	mm^2/s	2.969	2.646
Dynamic viscosity	Pa·s	2.47×10^{-3}	2.06×10^{-3}
Cetane number	-	54.6	79.6
Monoaromatic	$\%v/v$	20.1	0.50
Polyaromatic	$\%v/v$	3.00	0
Total aromatic	$\%v/v$	23.1	0
Flammability	°C	74.0	60.5
Lower heating value	MJ/kg	42.65	44.35
Hydrogen	%m/m	13.72	15.00
Carbon	%m/m	85.67	85.00
Oxygen	%m/m	0.61	0
Sulphur	mg/kg	6.50	0.53
FAME	$\%v/v$	5.00	0.05
Approx. formula	-	$C_{13}H_{24}O_{0.06}$	$C_{13}H_{28}$

2.3. Exerimental Test Procedure

The experimental campaign consisted of two distinct types of tests, each of which was intended to investigate the behavior of the engine running on HVO or diesel under different boundary conditions. In the first test type (test type #1), the engine is warmed up to 85 °C from a cold start and the baseline diesel-oriented calibration of the ECU is left unchanged for both fuels. In the second test type (test type #2), single-parameter sweeps are performed to determine how variations to some of the most important calibration parameters affect exhaust emissions and engine performance when running on either fuel. Separate descriptions of both test procedures are provided below.

2.3.1. Test Type #1: Warm-Up/Cool-Down Ramps

For test type #1, a cold engine is required. Before each test series, the engine was, therefore, soaked at room temperature overnight (at least 12 h). After properly warming

up all measuring devices (e.g., the emission analyzers), the engine was started, idled for a few seconds, and was then brought to the desired steady-state engine operating point. The engine was then allowed to "naturally" warm up until the coolant temperature at the engine outlet reached the nominal set value of 85 °C. At this point, the engine coolant temperature was "artificially" decreased by regulating the amount of water (from the laboratory facilities) flowing through the coolant water cooler using a PID-controlled electrovalve. The procedure was repeated for both fuels on two steady-state engine operating points, with rotational speeds of 1250 and 2000 rpm and brake mean effective pressure (*bmep*) values of 2 and 9 bar, respectively. They will be referred to as 1250 × 2 and 2000 × 9 from here on out. At each engine operating point, constant engine speed and *bmep* values were maintained by letting the engine test bench controller adjust the injected fuel supply accordingly.

The baseline (diesel-oriented) calibration of the engine remained unchanged throughout the entire test series. This means that the engine was free to operate with all of its actuations, strategies, and corrections as if no calibration tools (i.e., ETAS INCA) were available at the test bench to potentially tune calibration parameters on-the-fly. This implies that some engine calibration setpoints (rail pressure, SOI_{Main}, ecc.) may vary slightly throughout the warm-up period, mostly due to the varying accelerator pedal positions required for the engine to produce constant *bmep.* In this way, it is possible to examine the differences in engine performance and emissions between conventional (petroleum-derived) diesel and HVO as a "drop-in" fuel, i.e., without adjusting the baseline calibration of the engine.

Figure 2 depicts the temporal evolution of the coolant temperature for the 1250 × 2 ramp. As can be seen, the engine is first "naturally" warmed up to 85 °C before the coolant temperature is "artificially" decreased to 40 °C. The color gradient from dark to light green represents the elapsed time along the ramps. Darker shades represent earlier time, lighter shades represent later time.

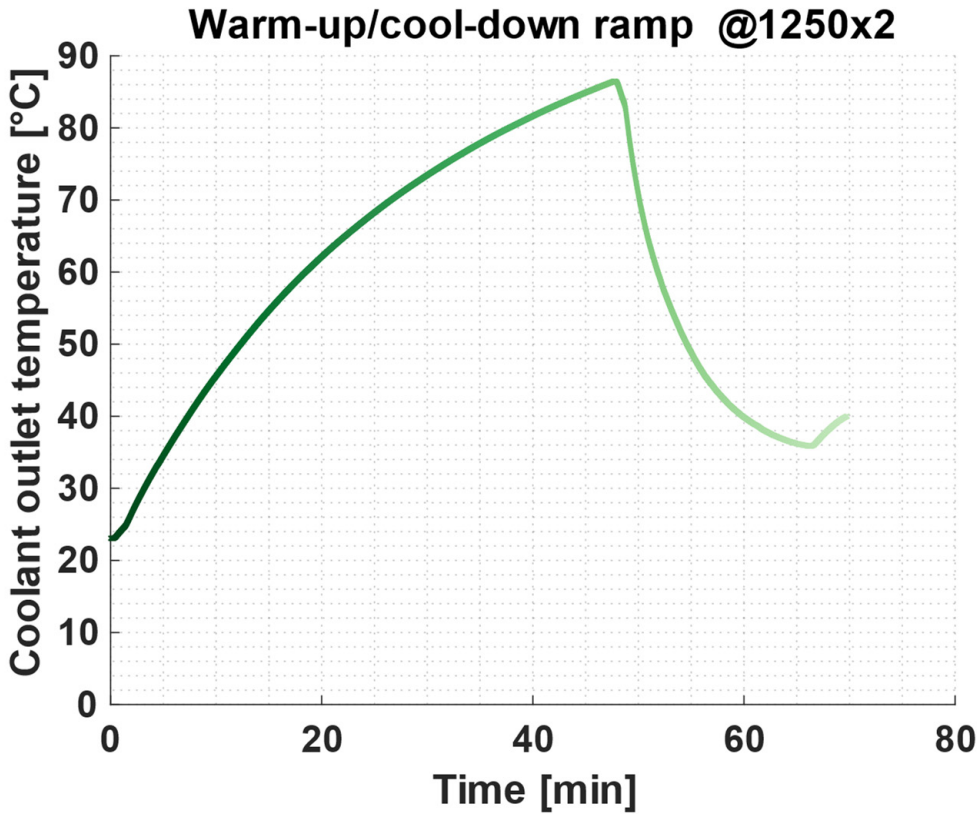

Figure 2. Evolution of the coolant temperature during a warm-up ramp at 1250 × 2. The dark-to-light green color palette is the function of the elapsed time and the same is used for Figure 3.

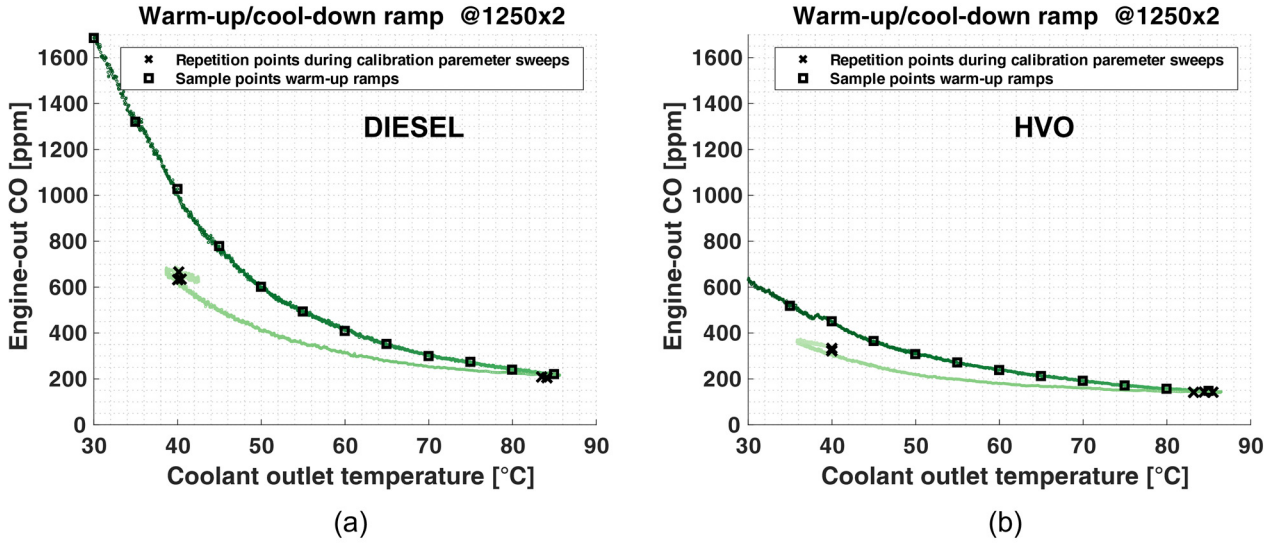

Figure 3. CO emissions for the 1250 × 2 ramp with diesel (**a**) and HVO (**b**) as a function of coolant outlet temperature. Dark and light green shades are the function of elapsed time (it is the same color palette as Figure 2). Black squared markers highlight data points used in the warm-up analysis in Section 3.1, whereas black cross markers highlight the results obtained by steady-state points acquired during the sweep-tests analysis in Section 3.2 and show test repeatability between ramps and sweeps.

2.3.2. Test Type #2: Calibration Parameter Sweeps

For test type #2, the effects of varying some of the main engine calibration parameters, i.e., rail pressure (p_{rail}), electric start of the main injection (SOI_{Main}), and intake in-cylinder air quantity (q_{air}), were studied for both diesel and HVO and for the same two engine operating points mentioned previously, at different coolant temperature values. Specifically, two steady-state temperature levels (40 °C and 85 °C at 1250 × 2 and 60 °C and 85 °C at 2000 × 9) were identified. Single-variable sweeps were performed at each coolant temperature level and with both fuels, that is, a "one-factor-at-a-time" approach, while keeping the others (including the boost pressure, which was not included in the parameter sweeps) fixed and equal for both fuels. Table 5 contains the main engine parameters used as "central points" throughout these variable sweeps. These values would have been (slightly) different if the original engine calibration had been let completely free (as in test type #1), depending on the specific fuel and on the actual coolant temperature, since the ECU applies some corrections to engine calibration parameters based on coolant temperature measurement (for example, it advances the fuel injection pattern if the coolant temperature declines). For a more meaningful comparison between fuels, each single-parameter sweep was carried out holding all the other parameters constant and fuel-independent. The objective was to examine differences in engine behavior attributable to fuel and coolant temperature only (isolating them as much as possible from potential calibration differences) as well as to analyze the engine response to specific changes in engine calibration parameters with both fuels, possibly identifying useful guidelines for engine recalibration during cold HVO operations.

Table 5. Setpoint values for the "central points" along calibration parameter sweeps. Setpoints are fuel independent.

	SOI_{Main}	p_{Rail}	q_{air}
	[°CA bTDC]	[mbar]	[mg/str]
1250 × 2 HOT	−2.8	610	316
1250 × 2 COLD	−1.4	570	316
2000 × 9 HOT	−2.4	1350	590
2000 × 9 COLD	−2.1	1320	595

2.3.3. Additional Observations on Experimental Test Procedures

It should be noted that because the ramps for test type #1 required overnight soaking, they had to be carried out at the start of different workdays (upon engine start). Sweep tests (test type #2), however, had to be performed with the engine running for several hours on the test bench for the remainder of the days, after one of the ramps pertaining to test type #1 had been completed.

Sweep tests with lower coolant temperatures (40 °C at 1250 × 2 and 60 °C at 2000 × 9) had to be carried out by keeping the coolant temperature "artificially" low for an extended period of time. This makes the results of low temperature sweeps inherently different from what could be obtained if the sweeps were performed on an engine running with the same coolant temperature, but just started up, primarily owing to the thermal inertia of the engine metal parts and different wall temperature gradients. However, this is the only test procedure that can achieve a proper degree of repeatability in low-temperature tests. That is to say, it would be impossible to carry out meaningful sweep tests while the engine is "naturally" warming up, because of the inherent transient behavior of such an operating condition.

The results from the ramps performed for test type #1 can help identify and quantify the differences, at the same coolant temperature, between a cold engine "naturally" warming up and an engine running on the test bench whose coolant water temperature is kept "artificially" low. Figure 3 depicts engine-out CO emissions as a function of coolant outlet temperature during the "natural" warm-up/"artificial" cool-down ramps at 1250 × 2, for diesel (Figure 3a) and HVO (Figure 3b). CO was selected as an example, but similar conclusions can be drawn from other pollutant emissions/combustion metrics, which are not reported here for conciseness reasons. The dark-to-light green color palette of Figure 3 is identical to that of Figure 2, allowing the elapsed time along the ramp to be derived from the same plot. Figure 3 highlights variations in the engine behavior at a same coolant temperature, depending on how that thermal level was reached (hysteresis pattern). Specifically, at the coolant outlet temperature approximately 40 °C during the first "natural" warm-up phase of the ramps, engine-out CO is around 1000 for diesel and 450 ppm for HVO, respectively, whereas, at the same coolant temperature, engine-out CO is around 650 and 350 ppm, respectively, if that temperature is "artificially" decreased and maintained low. These latter conditions are, incidentally, exactly how the low-temperature sweep tests (test type #2) were carried out.

In Figure 3, the black cross-shaped symbols (referred to as "repetition points" in the legend) represent the baseline calibration points around which the sweep tests were conducted (at low and high coolant temperatures). They are numerous because they represent repetition steady-state tests ("central points") carried-out during the test type #2 phase in order to assess the consistency and variability of these tests. As can be seen, black cross-shaped symbols referring to low coolant temperature "central points" overlap the end of the "artificial" cool-down portion of test type #1 ramps, whereas symbols referring to high coolant temperature "central points" overlap the "warmed-up" engine portion of the same ramps, suggesting that the engine thermal state during these tests is comparable.

Figure 3 also includes black square-shaped symbols (referred to as "sample points" in the legend) that represent sampled points extracted from the ramps (during the "natural" warm-up phase), which will be used in the following sections to analyze the results of test type #1.

3. Experimental Test Analysis

3.1. HVO vs. Conventional Diesel Oil: "Natural" Warm-Up Operation (Test Type #1)

Based on the previously described test procedure, this section analyzes the results in terms of exhaust emissions and engine performance during "natural" warm-up operation. As stated previously, the engine was run on either diesel or HVO while allowing its standard baseline calibration to run free. For each ramp performed, several data points, one every 5 °C, were sampled during the "natural" warm-up phase and will be shown in the following Figures 4–6.

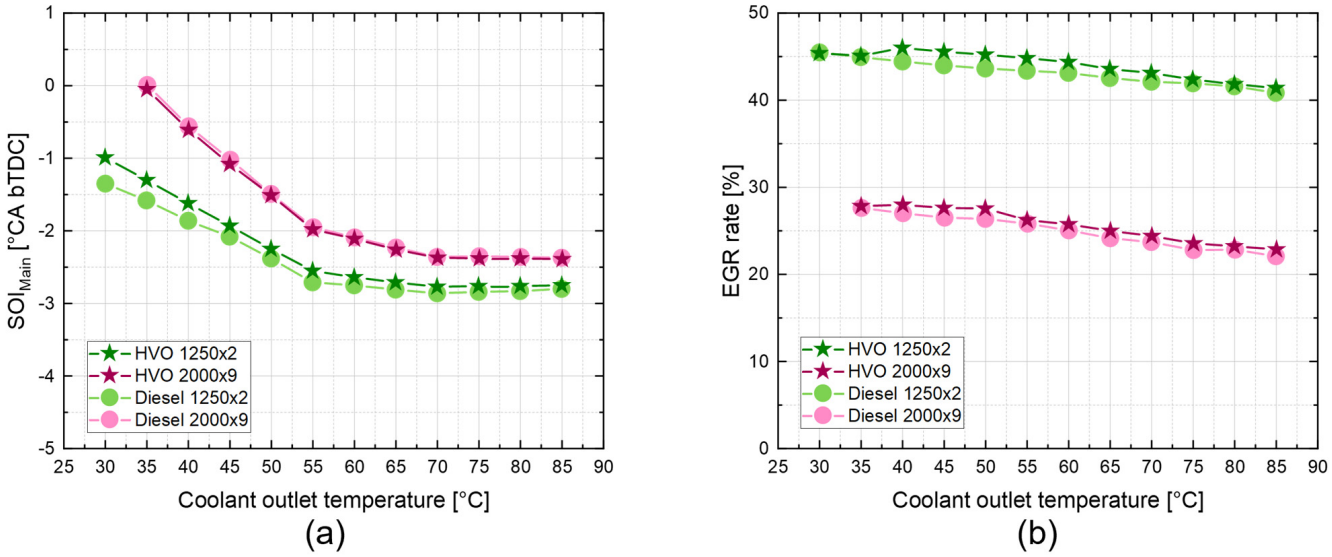

Figure 4. SOI$_{Main}$ (**a**) and EGR rate (**b**) measured at various coolant temperatures along the "natural" warm-up ramps of the engine. Comparison between diesel and HVO at 1250 × 2 and 2000 × 9. Light and dark greens represent 1250 × 2, pink and purple represent 2000 × 9. Circles represent diesel, while stars represent HVO.

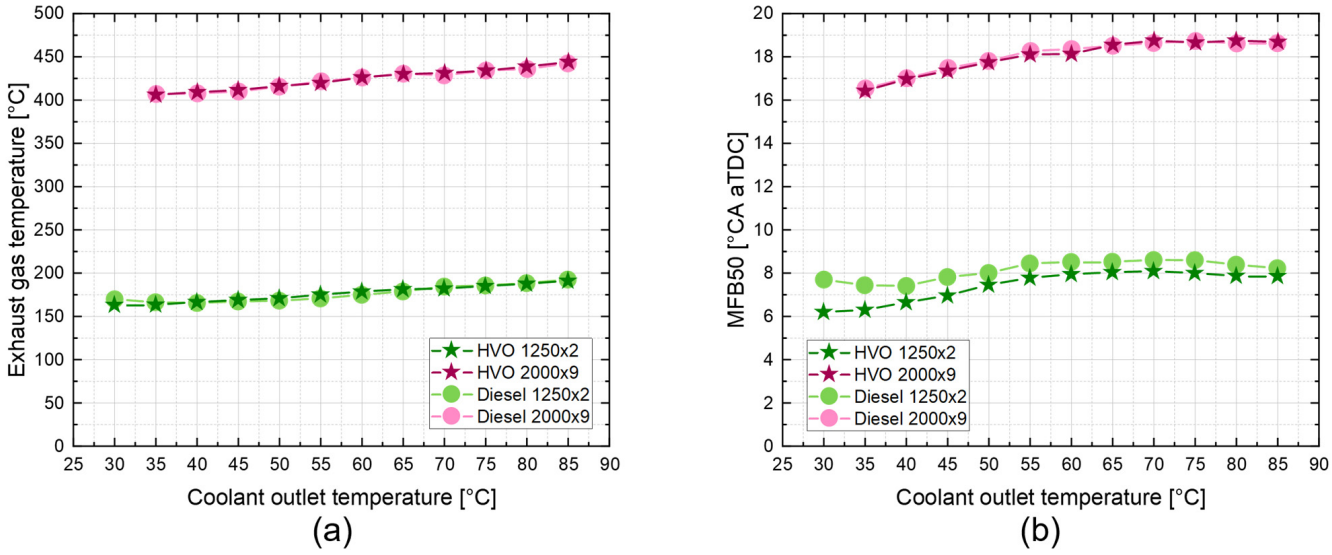

Figure 5. Exhaust gas temperature (**a**) and MFB50 (**b**) measured at various coolant temperatures along the "natural" warm-up ramps of the engine. Comparison between diesel and HVO at 1250 × 2 and 2000 × 9. Light and dark greens represent 1250 × 2, pink and purple represent 2000 × 9. Circles represent diesel, while stars represent HVO.

Before proceeding with the results analysis, a brief description of how the following figures display the outcomes of the "natural" warm-up tests is provided. A circle denotes diesel tests, while a star denotes HVO tests. The color distinction makes the coolant temperature at which the tests were performed visually intuitive. Light and dark greens represent 1250 × 2, pink and purple represent 2000 × 9.

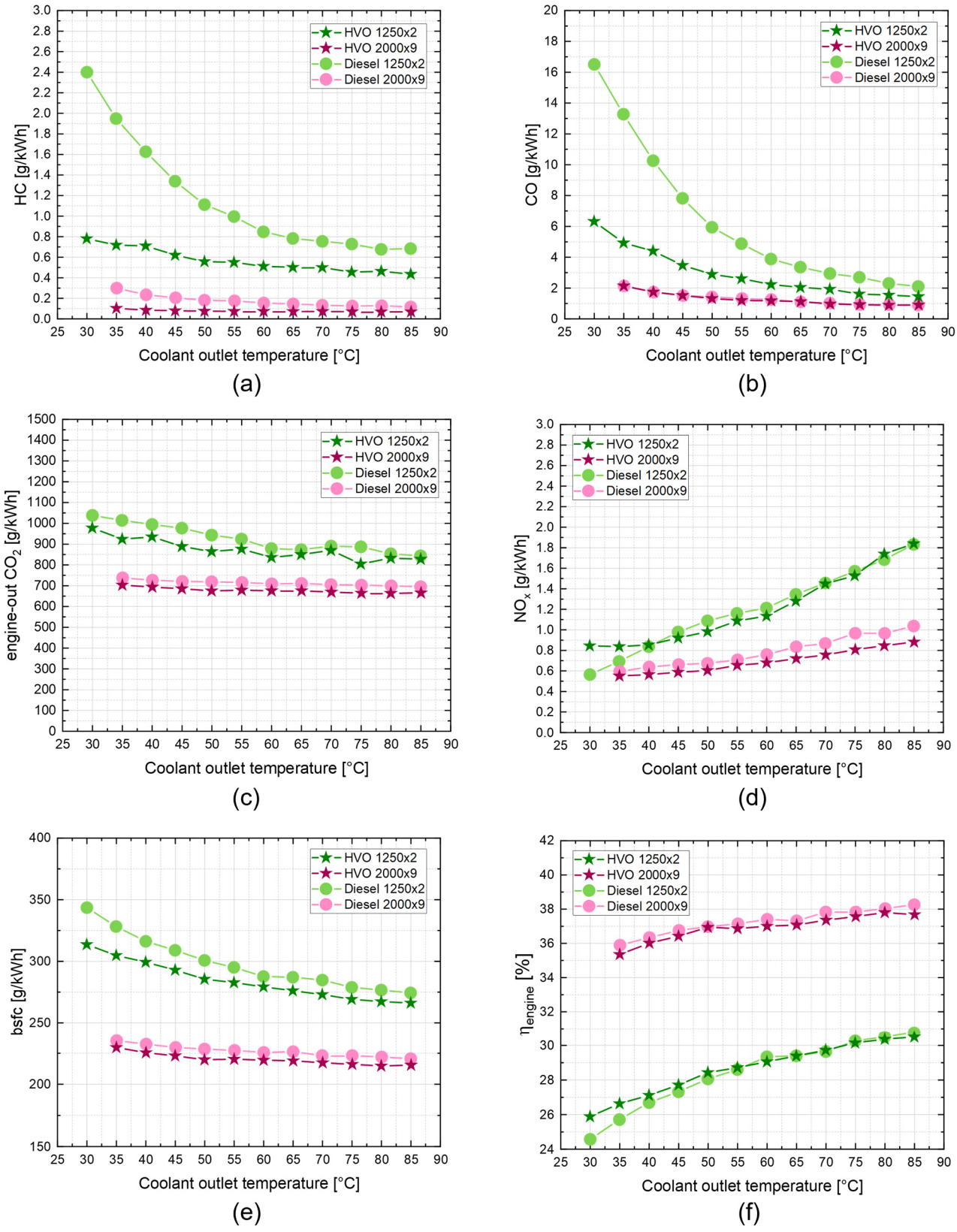

Figure 6. HC emissions (**a**), CO emissions (**b**), CO_2 emissions (**c**), NO_x emissions (**d**), *bsfc* (**e**) and engine thermal efficiency (**f**) measured at various coolant temperatures along the "natural" warm-up ramps of the engine. Comparison between diesel and HVO at 1250 × 2 and 2000 × 9. Light and dark greens represent 1250 × 2, pink and purple represent 2000 × 9. Circles represent diesel, while stars represent HVO.

3.1.1. Effects on Engine Combustion

During warm-up operation, engine combustion is not only affected by lower temperatures, but also by variations in ECU calibration parameters. The accelerator pedal position set by the test bench controller for the engine to produce constant *bmep* varies as a result of the increasing thermal efficiency of the engine as it warms up and of differences in fuel behavior. Consequently, some engine calibration setpoints change slightly during the warm-up phase. In addition, the ECU makes calibration corrections to compensate for lower coolant temperatures. For example, as can be observed in Figure 4a, which shows the variation of SOI_{Main} along the two warm-up ramps, the ECU tends to advance injection timings at low coolant temperatures to compensate for lower in-cylinder temperature at the time of injection, delayed combustion evolution caused by longer ignition delays and higher gas-wall heat exchanges.

The increase in coolant temperature along the "natural" engine warm-up is accompanied by an increase in exhaust gas temperature (cf. Figure 5a). The main reason for this should be related to decreasing gas-wall heat exchange as coolant temperature rises. Moreover, delayed combustion phasing may increase exhaust temperatures. However, as is evident in the 1250 × 2 diesel ramp, combustion at coolant outlet temperatures of 30 °C and 85 °C exhibits nearly the same combustion barycenter (represented by MFB50 values, which are around 8 °CA aTDC, cf. Figure 5b) but different exhaust temperatures, indicating that the primary factor influencing exhaust temperature is, in fact, heat transfer. MFB50 values at 2000 × 9, however, are not constant but exhibit monotonic delaying trends as coolant temperature rises, for both diesel and HVO. This is primarily caused by SOI_{Main} corrections implemented by the ECU as coolant temperature varies (MFB50 delay patterns are very similar to SOI_{Main} delays, cf. Figures 4a and 5b) and there is no substantial difference in behavior between HVO and diesel in this regard. In contrast, at 1250 × 2, HVO has a more advanced combustion barycenter than diesel. Moreover, even though SOI_{Main} corrections along the ramps are nearly the same for the two fuels, combustion barycenter advance with HVO is more pronounced at the lowest coolant temperatures (at coolant outlet temperature of 30 °C, for example, it has a combustion barycenter advanced by around 2 °CA compared to diesel). Despite the fuel injection advance at low coolant temperature, diesel features nearly constant MFB50 values around 8 °CA aTDC at 1250 × 2 (cf. Figure 5b). Nevertheless, SOI_{Main} advance fully translates into MFB50 advance for HVO, presumably due to its greater ignitability. This suggests that HVO is less susceptible to ignition delays at low coolant temperatures than diesel. Thus, a dedicated HVO calibration at low coolant temperatures would presumably require smaller SOI_{Main} corrections than conventional diesel.

3.1.2. Effects on Exhaust Pollutant Emissions and Engine Performance

Before delving into exhaust pollutant emissions and engine performance analyses, it is important to reiterate that SOI_{Main} is gradually delayed by the ECU as coolant temperature rises along the "natural" warm-up ramps. Furthermore, as shown in Figure 4b, the EGR rate decreases (as a result of changing engine thermal state) while the engine warms up, influencing the subsequent results.

HC and CO Emissions

As depicted in Figure 6a, lowering coolant temperatures increases HC emissions to a great extent, with both diesel and HVO. This is most likely due to an enhancement to overleaning and flame quenching phenomena, as in-cylinder and wall temperatures decline with colder thermal states, as these are two common mechanisms that cause HC emissions in diesel engines [8]. Furthermore, low temperatures may also inhibit HC oxidation in the cylinder and at the exhaust. It can be seen that a coolant temperature of 30 °C during the cold start of the 1250 × 2 diesel ramp corresponds to an HC emission level of 2.4 g/kWh, which is more than three times the value at 85 °C (0.68 g/kWh). HVO, however, experiences a significantly smaller increase in engine-out HC as coolant temperature is dropped, rising from 0.43 to just under 0.78 g/kWh. This is likely due to its enhanced ignition properties,

and similar conclusions can be drawn for the 2000 × 9 ramps. In fact, HVO emits less engine-out HC than diesel regardless of engine operating point and coolant temperature.

In terms of CO emissions (Figure 6b), HVO outperforms diesel along the 1250 × 2 ramps regardless of coolant temperature. At 85 °C, HVO reduces CO emissions by around 30% compared to diesel, from 2.10 to 1.45 g/kWh. At 30 °C, the advantage of HVO increases to 60%, reducing CO emissions from 16.5 to 6.32 g/kWh. In contrast, at 2000 × 9, the relative change in CO between HVO and diesel tends to be negligible, as do their absolute values, which are relatively low due to the high in-cylinder temperatures involved in the combustion process at this higher load.

In general, HVO reduces emissions from incomplete combustion due to its high cetane number and narrow distillation range, which improve ignition behavior. In compression ignition engines, fuel evaporation is critical, especially at low load and during cold start operation. Typically, fuels with low distillation curves, such as HVO, exhibit improved evaporation (hence mixing) with the intake charge and higher reactivity, particularly at low combustion temperatures [44]. Indeed, the more pronounced HC reduction brought about by HVO is clearly obtained at 1250 × 2 and coolant outlet temperature of 30 °C (−67% compared to diesel). When the engine is warmed-up, however, the reduction is less pronounced in relative terms, as HC emissions are cut by 37%. HVO still outperforms diesel at 2000 × 9, but HC emissions at this higher load are generally lower for both fuels (below 0.3 g/kWh), diminishing the significance of the differences.

It is worth noting that the discussed effects of fuel properties and coolant temperature on HC and CO emissions outweigh any other possible effect of variations in engine and calibration parameters along the ramps (e.g., SOI_{Main} and EGR rate). Progressive delays in SOI_{Main} (cf. Figure 4a) as the engine warms up would, if anything, contribute to the opposite direction of the visible HC and CO trends. In contrast, EGR rate reduction (cf. Figure 4b) as coolant temperature rises would be consistent with the declining trends of HC and CO. However, if reference is made to the 1250 × 2 ramps, the EGR rate at 30 °C and 35 °C coolant temperatures is relatively flat and comparable for the two fuels, yet their HC and CO emissions are significantly different.

NO_x Emissions

In addition to a predictable increase in NO_x emissions with increasing load for both fuels, Figure 6d indicates that NO_x emissions increase with rising coolant temperatures as well. Hotter coolant results in an increase in in-cylinder gas temperatures due to a decrease in heat transfer between in-cylinder gases and wall, both in the compression phase (leading to higher compressed gas temperatures at the onset of combustion) and during combustion (leading to higher in-cylinder peak combustion temperatures, which are highly correlated with NO_x formation mechanisms along with intake O_2) [45,46].

Regarding differences between fuels, NO_x emission levels of HVO and diesel appear comparable. As a function of coolant outlet temperature, there is no discernible trend indicating that one fuel emits consistently more (or less) NO_x than the other. This is consistent with the existing literature on the subject [22,30], which suggests that it is still uncertain whether HVO decreases or increases NO_x emissions relative to diesel. The higher the cetane number, the shorter the ID and the faster the combustion. However, a shorter ID does not necessarily guarantee NO_x reduction [47], and results may vary depending on the actual engine load, coolant temperature, and/or calibration-specific parameters. Specifically, NO_x variations appear to be much more influenced by EGR variations than any other parameter, and this will be discussed in greater detail based on the results of test type #2.

Fuel Consumption and Engine Thermal Efficiency

In addition to the previously observed reductions in engine-out pollutant emissions, Figure 6e shows how, due to its higher heating value (44.35 vs. 42.65 MJ/kg, cf. Table 4), HVO also reduces brake specific fuel consumption (*bsfc*) in comparison to the reference diesel fuel. The same plot also demonstrates that *bsfc* is worse at low coolant temperatures

because of increased friction and less efficient combustion (details on this aspect and the effects of oil and coolant water temperatures on frictions have been thoroughly studied in [48]). Similar conclusions can be drawn from Figure 6f, which depicts engine thermal efficiency (η_{engine}) as a function of coolant outlet temperature. For both fuels, η_{engine} is better at warmed-up coolant temperatures and worse at reduced coolant temperatures. However, owing to its increased reactivity and ignitability, which allows HVO combustion to develop faster even during cold starts, the efficiency drop of HVO at low coolant temperatures is less pronounced than that of diesel, particularly at low load. For the 1250 × 2 ramps, HVO is nearly 2% more efficient than diesel at 30 °C coolant outlet temperature, with this benefit declining as the engine warms up. When the engine has warmed up, the trend flips over, with diesel displaying higher efficiency than HVO, albeit very slightly (+0.2%). For the 2000 × 9 ramps, η_{engine} turns out to be slightly higher for diesel along the whole ramp, and efficiency degradation as coolant temperature decreases turns out to be less for both fuels.

Finally, as shown in Figure 6c, even when η_{engine} of HVO is lower than that of diesel due to the differences in chemical properties and heating value of the two fuels, engine-out CO_2 emissions are comparable or slightly lower for HVO. Nevertheless, the real potential of HVO in terms of CO_2 emission reduction in the atmosphere is not directly linked to engine-out CO_2 (i.e., tank-to-wheel CO_2) but has to be estimated through a well-to-wheel analysis, considering HVO is produced from renewable feedstocks that absorb CO_2 while growing [4].

3.2. HVO vs. Conventional Diesel Oil: Calibration Parameter Sweep Tests (Test Type #2)

This chapter examines the results in terms of exhaust emissions and engine performance along calibration parameter sweeps, based on the test procedure #2 described in Section 2.3.2. Sweep tests were performed at 1250 × 2 with coolant outlet temperatures of 40 °C (for cold conditions) and 85 °C (for warmed-up conditions), but at 2000 × 9 the coolant temperature could not be reduced below 60 °C for cold conditions (due to insufficient cooling power of the test bench heat exchanger). Warmed-up coolant temperature did not change (85 °C). It is worthwhile repeating that, since these sweep tests were carried out by "artificially" controlling the coolant outlet temperature, they are inherently unable of capturing all the effects that occur during a natural warm-up of the engine. Nevertheless, they can still be thought as representative of drawbacks an engine would endure at colder thermal states compared to warmed-up conditions.

To investigate the effects of the selected calibration parameters (SOI_{Main}, p_{rail} and q_{air}) one at a time, single-parameter sweeps were carried out, while keeping fixed the setpoints values for all the other parameters (in addition to fixed boost pressure, which was not included in the sweeps). These setpoint values were retrieved from the baseline calibration of the engine and made equal for HVO and diesel, as shown in Table 5.

Before proceeding with the results analysis, a brief description of how the following figures display the outcomes of the sweep tests is provided. A circle denotes diesel tests, while a star denotes HVO tests. The color distinction makes the coolant temperature at which the tests were performed visually intuitive. Blue and cyan (cool colors) represent low coolant temperature tests (40 °C at 1250 × 2, 60 °C at 2000 × 9), while red and orange (warm colors) represent high coolant temperature tests (85 °C). Black-edged symbols represent the "central point" (referring to the fixed baseline calibration, cf. Table 5) around which the sweeps were carried out.

3.2.1. SOI_{Main} Sweep

Combustion phasing is a crucial calibration parameter and has a direct influence on fuel consumption, pollutant emissions, and global engine performance. It is normally set to obtain the lowest possible *bsfc* (for a given braking power) while ensuring engine-out pollutant emissions stay below reasonable limits and/or engine performance does not degrade. In this Subsection, SOI_{Main} sweeps were carried out (i.e., SOI_{Main} was advanced or delayed relative to the baseline value) to investigate how adjusting combustion phasing may result in different outcomes for both investigated fuels, taking into consideration their distinct features.

Engine-Out HC and CO Emissions

As shown in Figure 7, HVO combustion produces significantly lower levels of CO and HC at the engine exhaust than diesel combustion, especially at low load, where this reduction is more interesting, due to potential low catalytic efficiency of after-treatment systems. At 2000 × 9, however HC levels are extremely low, for both fuels, while CO levels remain appreciable and exhibit a clear "u-shaped" trend as a function of SOI_{Main}. When SOI_{Main} is too delayed, a greater amount of fuel misses the piston bowl (the spray trajectory is too wide to enter the bowl, due to the distant position of the piston at the time of the main injection) and is injected towards the cylinder walls and the piston head, near the squish region [34]. This results in inefficient use of the oxygen present within the piston bowl volume, contributing to CO emissions. Furthermore, delayed injection timings reduce the amount of time available to complete CO oxidation reactions at the end of the expansion stroke. However, when a significant portion of the injected spray is targeted on the piston surface and splits evenly into two parts, one entering the squish region and the other entering the piston bowl, thus optimizing oxygen usage, a minimum in CO trends as a function of SOI_{Main} can be detected [49]. At 1250 × 2 this "u-shaped" CO trend is less evident, presumably because of higher in-cylinder oxygen availability at low load, which makes this phenomenon contribute less to CO formation [8].

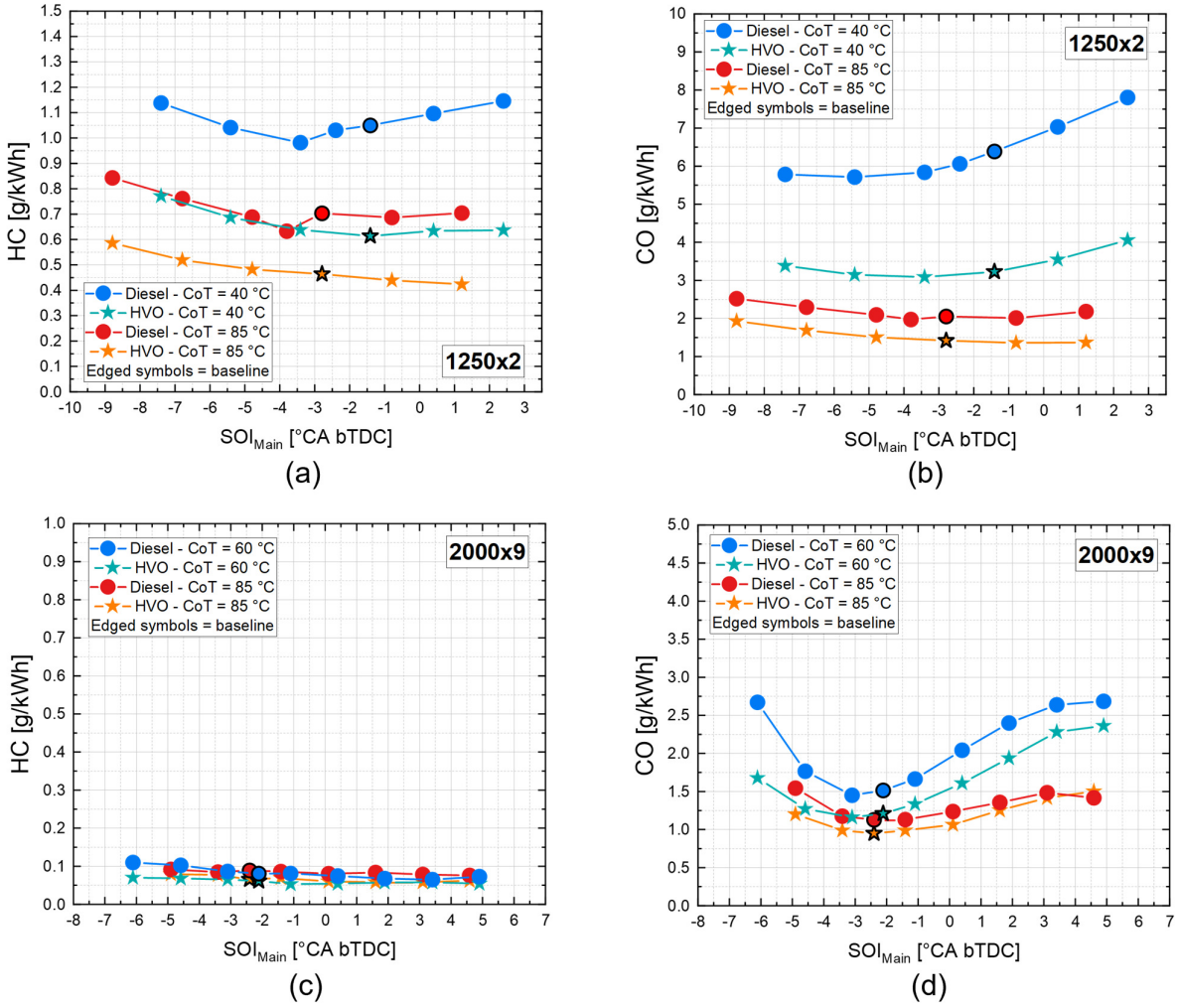

Figure 7. Engine-out HC and CO emissions along SOI_{Main} sweep tests at 1250 × 2 (**a**,**b**) and 2000 × 9 (**c**,**d**). Comparison between diesel and HVO at high and low coolant temperatures. Warm colors (red and orange) represent high coolant temperatures, while cool colors (blue and cyan) represent low coolant temperatures. Circles represent diesel, while stars represent HVO.

HC and CO reduction provided by HVO is certainly noticeable in warmed-up conditions (within 20 to 30% at 1250 × 2, even below 10% at 2000 × 9), but it is even more significant at lower coolant temperatures, with diesel generating up to twice as much CO as HVO along the whole SOI_{Main} sweep at 1250 × 2. In terms of CO, not only does diesel have higher overall emission values, but it also appears to be more sensitive to SOI_{Main} variations than HVO, particularly at low coolant temperatures, with more pronounced diverging trends as the injection pattern is advanced. For example, at 1250 × 2, an injection advance from −7 to 2 °CA bTDC results in a 33% CO increase (from 6 to 8 g/kWh), whereas the same SOI_{Main} variation for HVO results in a 14% CO increase (from 3.5 to 4 g/kWh only).

Engine-Out NO_x and Soot Emissions

As shown in Figure 8, HVO consistently outperforms diesel in terms of soot emissions, regardless of combustion phasing and coolant temperatures. As a function of SOI_{Main}, both fuels exhibit similar soot trends. At 1250 × 2, there is a slight soot increase at first as SOI_{Main} is advanced from very delayed values, followed by a gradual decrease as combustion is further advanced. At 2000 × 9, however, trends of soot emissions are similar to trends of CO, with a "u-shaped" minimum particularly visible especially at low coolant temperatures. This implies that similar explanations, related to improved air-fuel mixing when the fuel spray properly targets the edge of the piston bowl, might still be valid for soot formation mechanisms, at higher load. It is interesting to note, however, how diesel at low coolant temperatures and high load produces significantly more soot than HVO (up to +50%), despite both fuels exhibit similar trends.

Soot formation is a complex phenomenon influenced by a number of factors, including fuel properties (cetane number, density, viscosity, and the presence of aromatic and polyaromatic compounds) and EGR rate. Because EGR rate does not vary significantly enough across the entire SOI sweeps to justify such large soot differences (because intake air flow rate and boost pressure are fixed at each coolant temperature value), smoke differences between HVO and diesel can be attributed almost entirely to their distinct fuel properties and the absence of aromatic chemical compounds (which tend to act as soot precursors) in HVO composition. In addition, compared to conventional diesel, HVO has a lower density and viscosity, as well as a narrower distillation temperature range, as stated in previous subsections. This presumably promotes faster evaporation and a more uniform air-fuel mixture throughout the fuel cloud [26], hence, further contributing to reduce soot formation. Nevertheless, the amount of soot produced at low load is generally small, so reduction in soot is of much more interest at 2000 × 9.

Engine-out NO_x levels are very similar for HVO and diesel, across all SOI sweep tests. Only when the engine is warmed up does HVO appear to emit slightly less NO_x than diesel, at both tested engine operating points. This slight difference may be attributable to minor EGR differences (reported, as an example, in Figure 9, at 2000 × 9) that can occur during testing, even if intake air flow rate and boost pressure are kept fixed. This is most likely because HVO produces lower exhaust gas temperatures than diesel, resulting in lower temperatures of the residual gas in the combustion chamber at the end of combustion, higher density of the gas recirculated in the intake manifold and a lower intake temperature. For very delayed SOI_{Main}, this results in an increase in EGR of about 2% for HVO, which presumably causes the abovementioned slight NO_x reduction. While this minor increase in EGR benefits HVO by lowering NO_x, it has little effect on HC, CO, or soot emissions, which are much more linked to the chemical properties of the fuel.

Engine Thermal Efficiency and Fuel Consumption

HVO shows lower *bsfc* than diesel across the entire SOI_{Main} sweeps (due to its lower heating value). Engine thermal efficiency, however, is very similar, as shown in Figure 10. In fact, advancing SOI_{Main} diesel seems to slightly outperform HVO, with this effect more evident at high coolant temperature. In contrast, for very delayed SOI_{Main}, the trend flips over, with HVO resulting in slightly higher efficiencies.

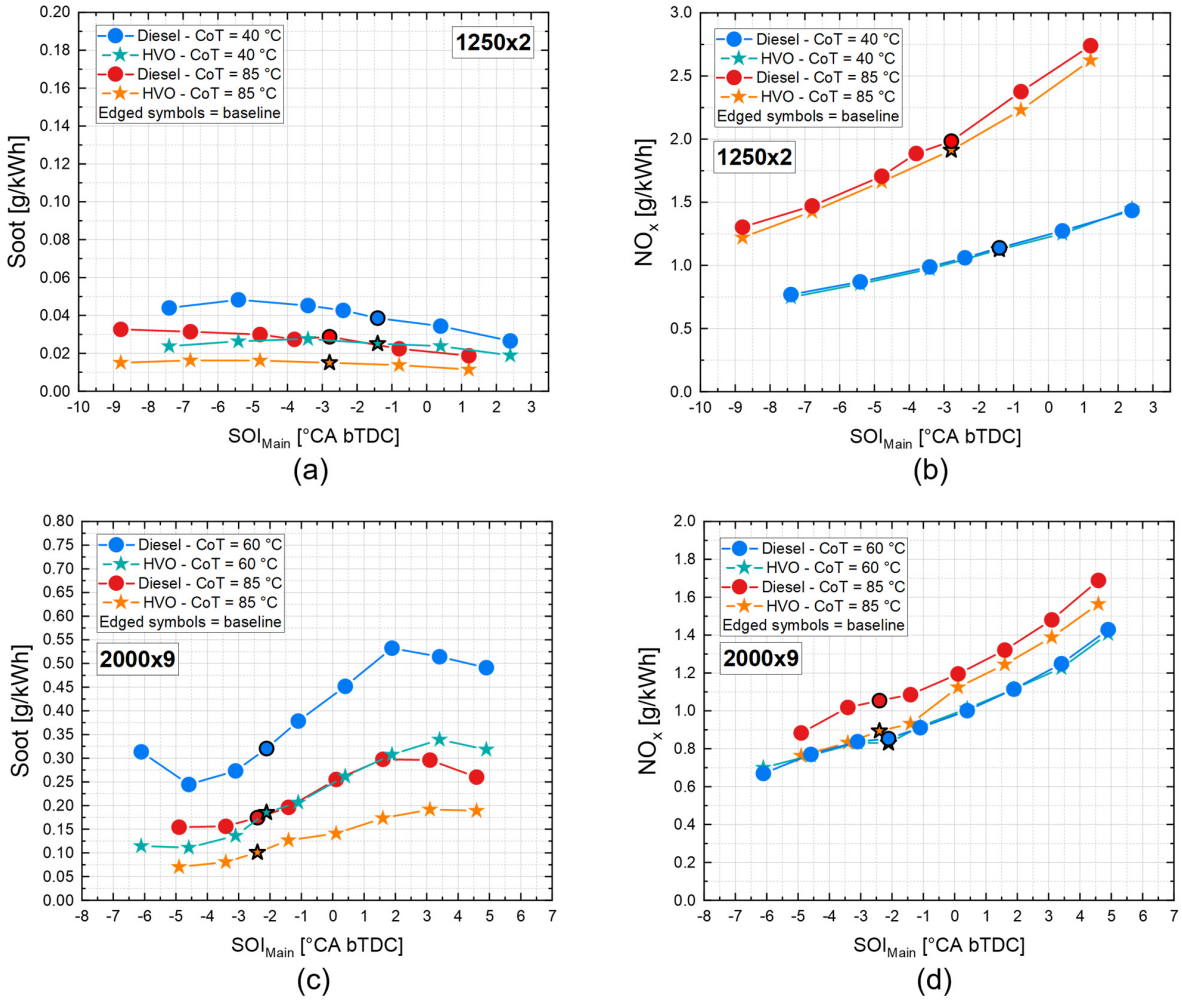

Figure 8. Soot and NO_x emissions along SOI_{Main} sweep tests at 1250 × 2 (**a**,**b**) and 2000 × 9 (**c**,**d**). Comparison between diesel and HVO at high and low coolant temperatures. Warm colors represent high coolant temperatures, while cool colors represent low coolant temperatures. Circles represent diesel, while stars represent HVO.

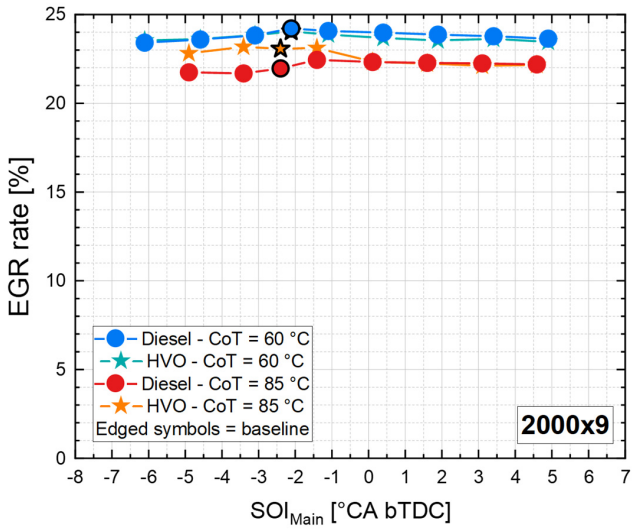

Figure 9. EGR rate along SOI_{Main} sweep tests at 1250 × 2 and 2000 × 9. Comparison between diesel and HVO at high and low coolant temperatures. Warm colors represent high coolant temperatures, while cool colors represent low coolant temperatures. Circles represent diesel, while stars represent HVO.

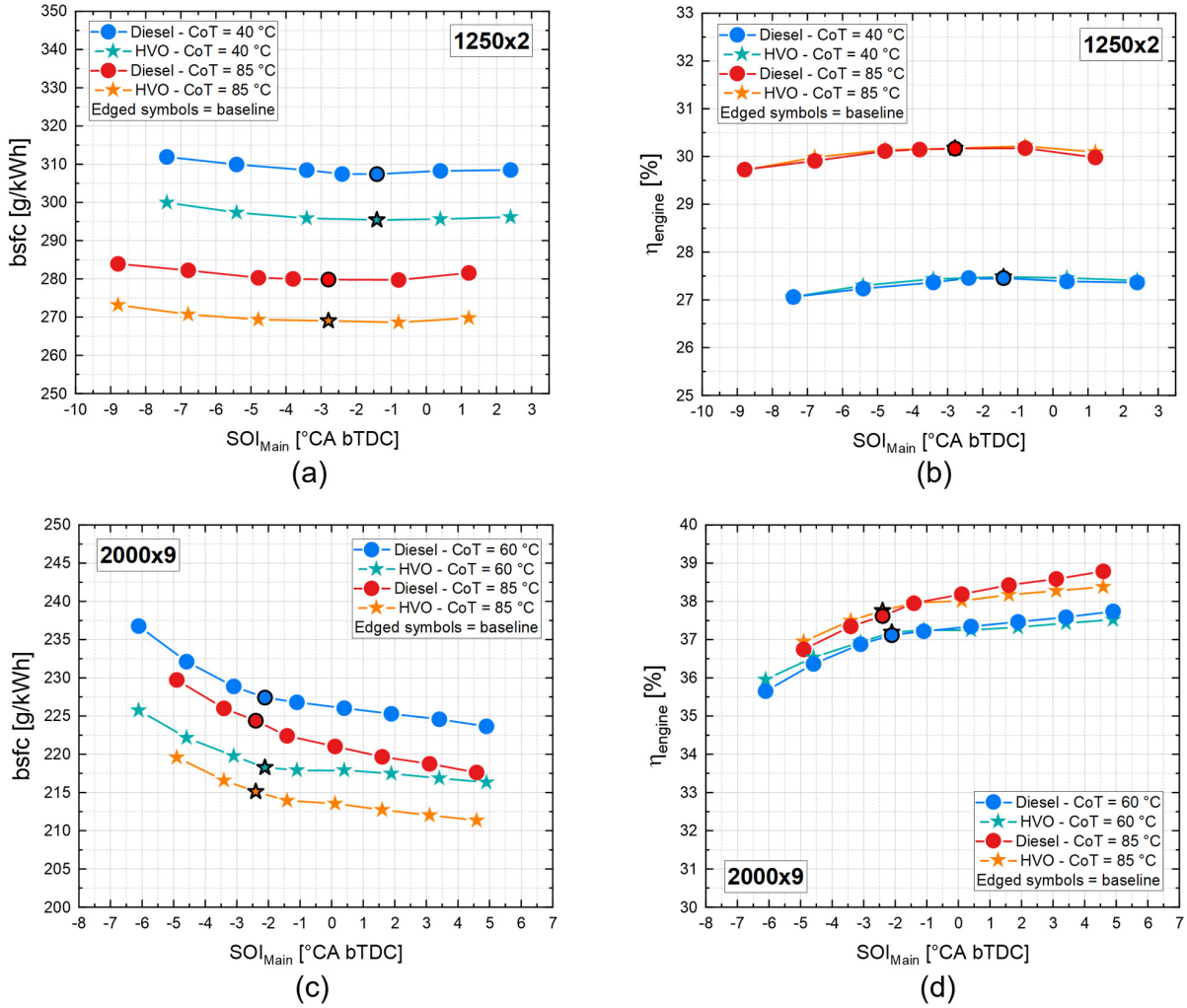

Figure 10. *bsfc* and engine efficiency along SOI_{Main} sweep tests at 1250 × 2 (**a**,**b**) and 2000 × 9 (**c**,**d**). Comparison between diesel and HVO at high and low coolant temperatures. Warm colors represent high coolant temperatures, while cool colors represent low coolant temperatures. Circles represent diesel, while stars represent HVO.

3.2.2. p_{Rail} Sweep

Rail pressure is a crucial calibration parameter that has a strong influence on air-fuel mixture formation, which results in a significant impact on engine-out pollutant emissions and engine performance. In this subsection, p_{Rail} sweeps carried out (i.e., p_{Rail} was increased or reduced relative to the baseline value) to investigate how adjusting rail pressure may result in different outcomes for both investigated fuels, taking into consideration their distinct features are presented.

Engine-Out HC and CO Emissions

As shown in Figure 11, confirming the results of previous subsections, engine-out CO and HC emissions from HVO combustion are significantly lower than conventional diesel regardless of fuel injection pressure, especially at low load. At 1250 × 2, HC (regardless of coolant temperature) and CO (in warmed up conditions) emissions are relatively unaffected by changes within investigated p_{Rail} ranges, with both diesel and HVO. However, at low coolant temperatures, HVO clearly highlights the tendency to maintain low sensitivity to changes in rail pressure, unlike diesel, which exhibits a substantial increase in this emission level. For example, Figure 11b shows that, at low coolant temperatures, increasing rail pressure from 400 to 800 bar generally increases CO emissions, most likely due to prevailing

over-leaning phenomena with improved fuel atomization [8]. However, the CO increase for diesel goes from 5.5 to 8 g/kWh, whereas only from 3 to 4 g/kWh for HVO.

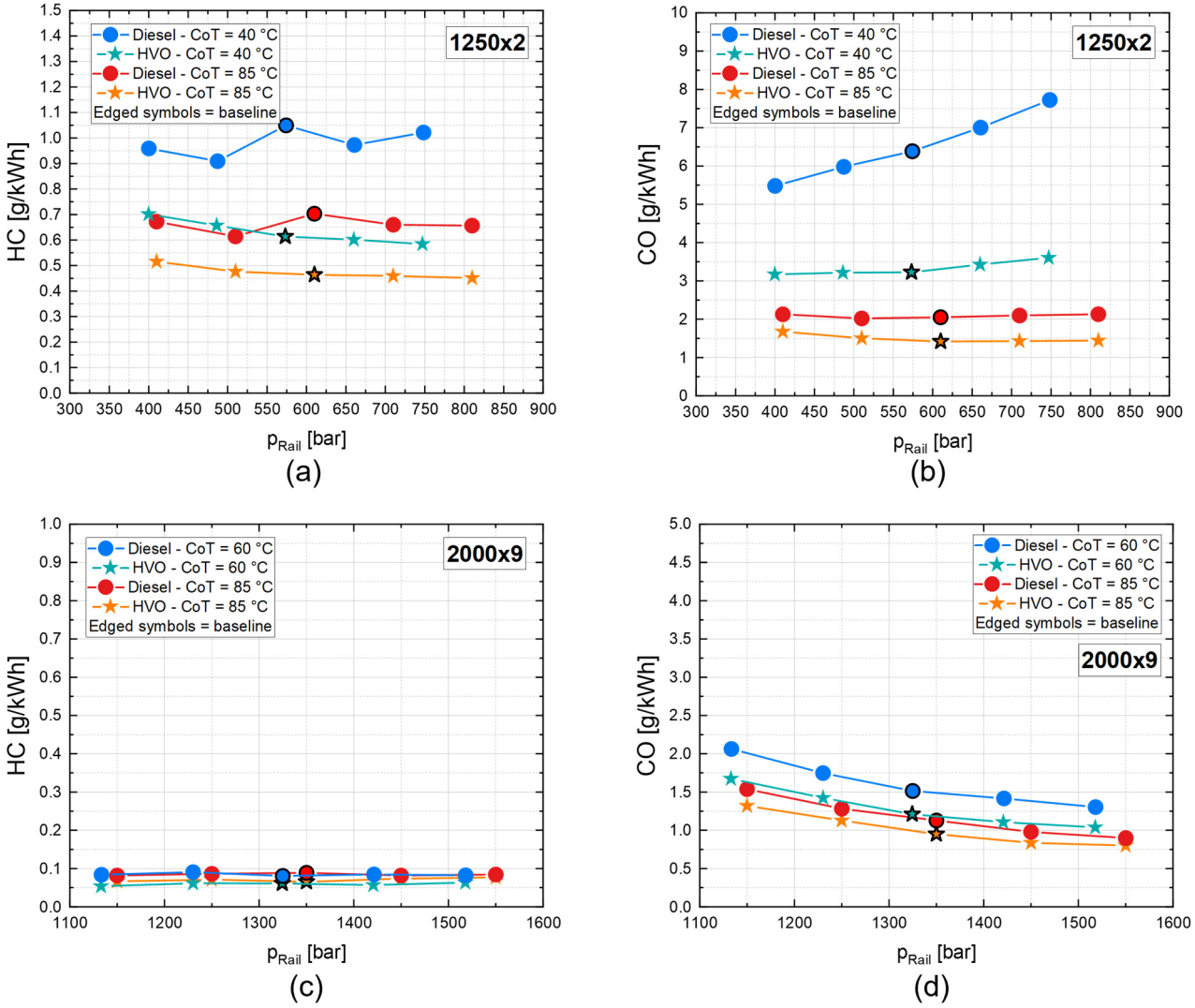

Figure 11. HC and CO emissions along p_{Rail} sweep tests at 1250 × 2 (**a**,**b**) and 2000 × 9 (**c**,**d**). Comparison between diesel and HVO at high and low coolant temperatures. Warm colors represent high coolant temperatures, while cool colors represent low coolant temperatures. Circles represent diesel, while stars represent HVO.

CO trends at 2000 × 9 differ from low load conditions, with increasing rail pressure resulting in decreasing CO emissions. At higher loads, increasing fuel injection pressure improves the air-fuel mixing, and since the dominant effect on CO formation at higher loads is linked to oxygen deficiency, this results in lower CO levels. Nevertheless, HVO still outperforms diesel as far as CO are concerned, while HC trends, throughout the trade-off, are negligible.

Engine-Out NO_x and Soot Emissions

As shown in Figure 12, NO_x and soot emissions are not only affected by engine loads and particular fuel used, but also by rail pressure variations. Increased p_{Rail} improves fuel atomization, enlarges the interface between fuel spray particles and air, and decreases evaporation time. As a consequence, the air entrainment into the fuel spray and the mixture formation process are greatly enhanced and the fuel distribution is more uniform. All of these factors hinder soot formation mechanisms. Furthermore, increased p_{Rail} results in

higher in-cylinder pressure and temperature values during combustion, which ultimately favor NO_x formation mechanism, setting up a clear NO_x/soot trade-off.

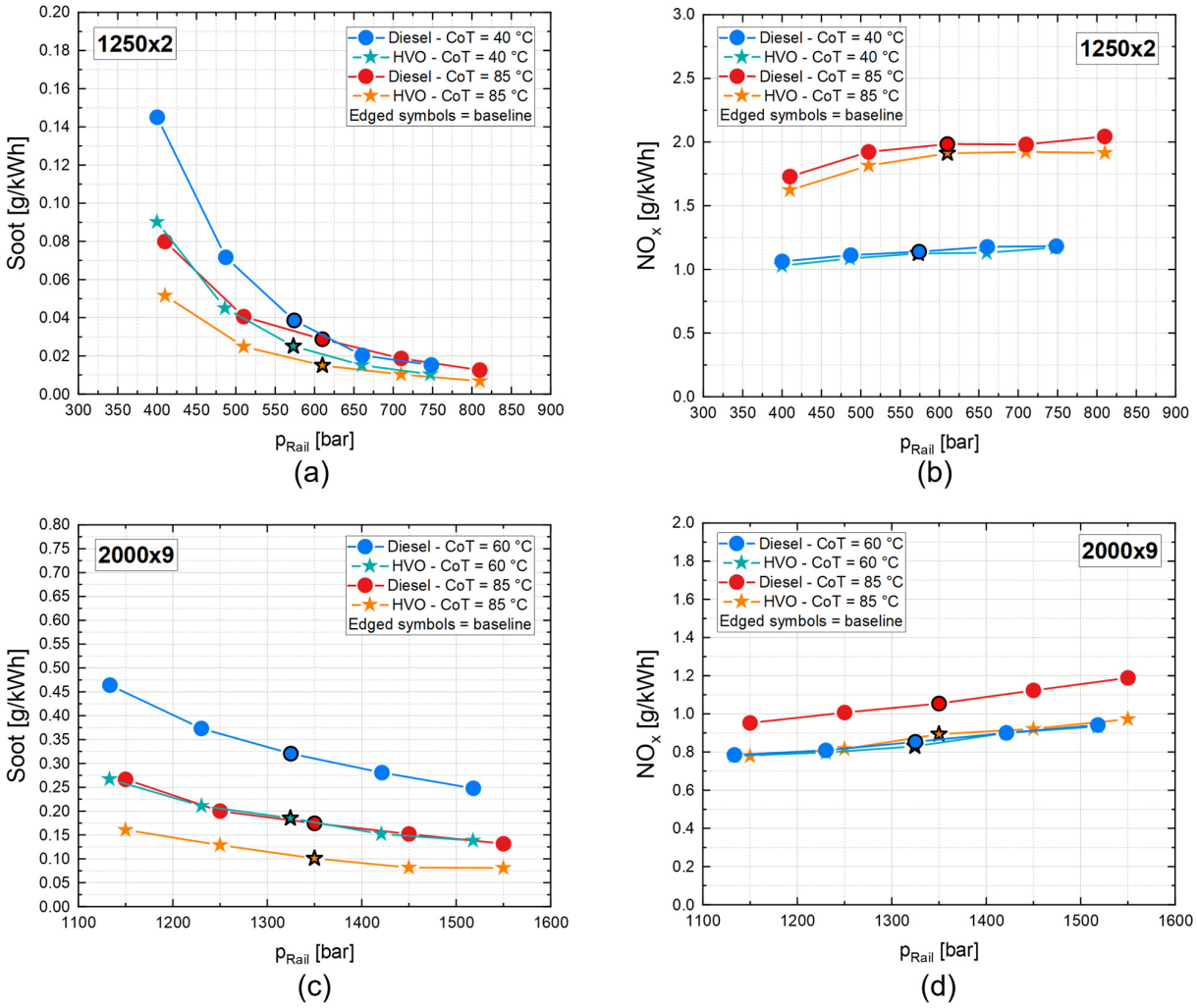

Figure 12. Soot and NO_x emissions along p_{Rail} sweep tests at 1250 × 2 (**a**,**b**) and 2000 × 9 (**c**,**d**). Comparison between diesel and HVO at high and low coolant temperatures. Warm colors represent high coolant temperatures, while cool colors represent low coolant temperatures. Circles represent diesel, while stars represent HVO.

As far as differences between fuels are concerned, NO_x variations can be mainly attributed to slightly different EGR levels across the tests (despite boost pressure and intake air quantity setpoints are kept constant), as discussed in the previous subsections. Regarding soot, if the highest rail pressure is maintained (800 bar), smoke levels at 1250 × 2 are bounded within a narrow range for all tests (diesel and HVO, hot and cold coolant). Conversely, at low coolant temperatures and low fuel injection pressure, HVO outperforms diesel once again, by up to 40%. This means that, at low coolant temperatures, diesel seems to be more sensitive to changes in fuel injection pressure than HVO. At 2000 × 9, HVO outperforms diesel across the entire p_{Rail} trade-off. Diesel soot levels increase from 0.25 to 0.45 g/kWh when starting from the highest rail pressure and decreasing it, whereas HVO levels increase from 0.15 to 0.27 g/kWh.

Engine Thermal Efficiency and Fuel Consumption

At 1250 × 2, engine efficiency is relatively unaffected by changes in rail pressure, at least within the investigated variation ranges (cf. Figure 13b). No differences are

visible between fuels. Distinct fuel properties (namely, lower heating value) justify the corresponding differences in *bsfc*. At 2000 × 9, however, an increase in rail pressure improves η_{engine} for both HVO and diesel, but again the two fuels perform similarly at each coolant temperature.

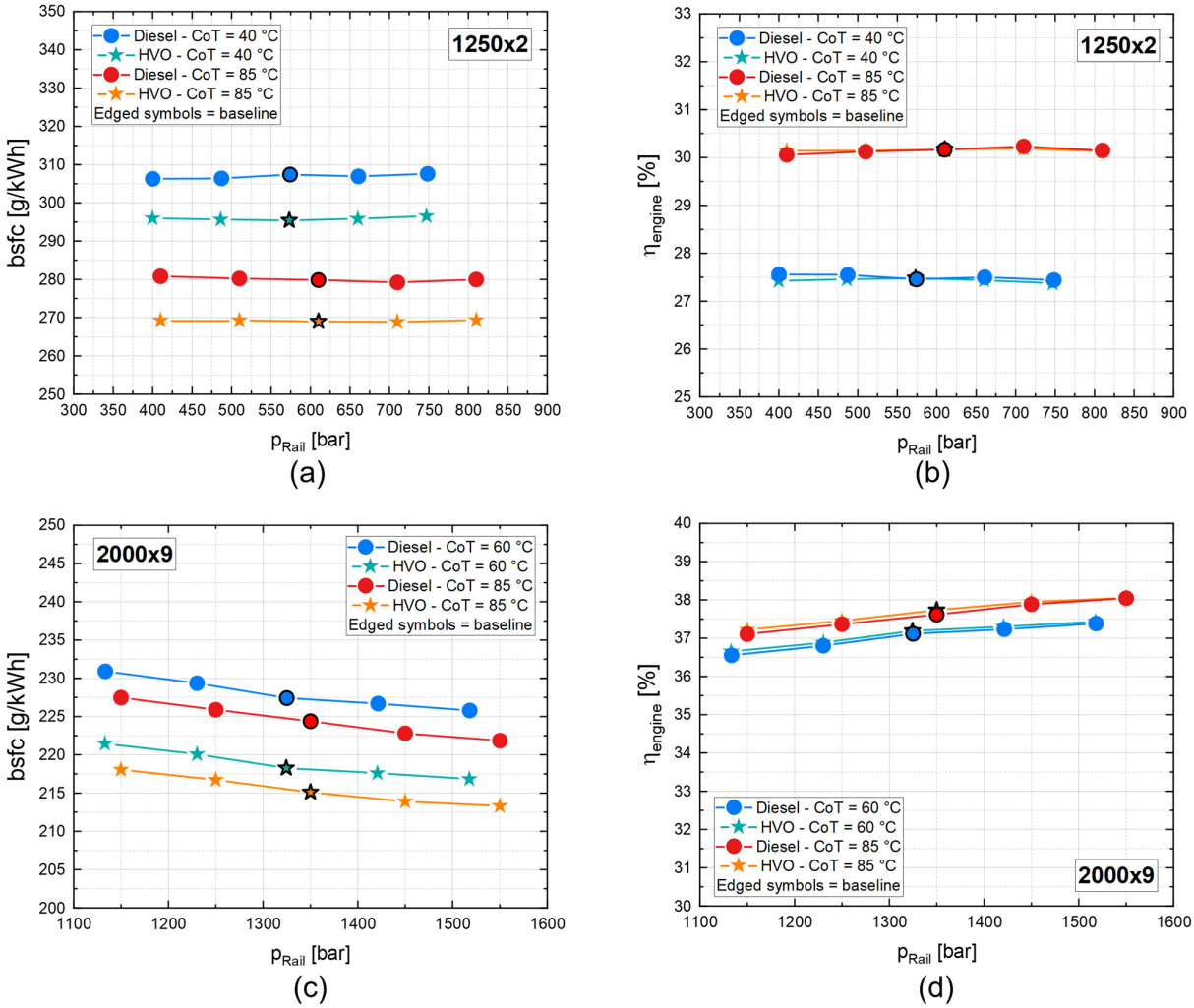

Figure 13. *bsfc* and engine efficiency along p_{Rail} sweep tests at 1250 × 2 (**a**,**b**) and 2000 × 9 (**c**,**d**). Comparison between diesel and HVO at high and low coolant temperatures. Warm colors represent high coolant temperatures, while cool colors represent low coolant temperatures. Circles represent diesel, while stars represent HVO.

3.2.3. q_{air} Sweep

Varying the intake air quantity is mostly used for hindering NO_x formation mechanisms in the cylinder. NO_x/CO and HC/CO trade-offs are generally of primary concern for lower loads, while at higher loads, NO_x-soot trade-off is more significant. In this subsection, q_{air} sweeps were carried out (i.e., q_{air} was increased or reduced relative to the baseline value) to investigate how varying intake air quantity (thus, EGR rate and intake oxygen) may result in different outcomes for both investigated fuels, taking into consideration their distinct features. The baseline value for the intake air sweep at 1250 × 2 features the minimum q_{air} (i.e., the highest EGR rate), since the engine baseline ECU calibration keeps the EGR valve fully open in order to reduce NO_x engine-out to the greatest extent. Therefore, at 1250 × 2, the intake air sweep was performed by gradually increasing the air setpoint, starting from the minimum (relative to the baseline setpoint) to its highest value (corresponding to a condition with the EGR valve fully closed, thus no EGR).

Engine-Out HC and CO Emissions

As shown in Figure 14, engine-out CO and HC emissions from HVO combustion are once again significantly lower than conventional diesel, regardless of EGR rate and coolant temperature, especially at low load. At 1250 × 2, HC and CO emissions show little variations within the tested intake air flow rate ($\dot{m}_{air}$) ranges, with both diesel and HVO. Diesel at low coolant temperatures and highest EGR rates is the only exception. HVO tends to maintain lower sensitivity to changes in calibration parameters compared to diesel, as previously discussed. For example, at low coolant temperatures decreasing $\dot{m}_{air}$ from 60 to 48 kg/h increases CO emissions, most likely due to worsened in-cylinder combustion as EGR rate rises. However, the CO increase for diesel goes from 4.8 to 6.5 g/kWh, whereas only from 2.8 to 3.2 g/kWh for HVO.

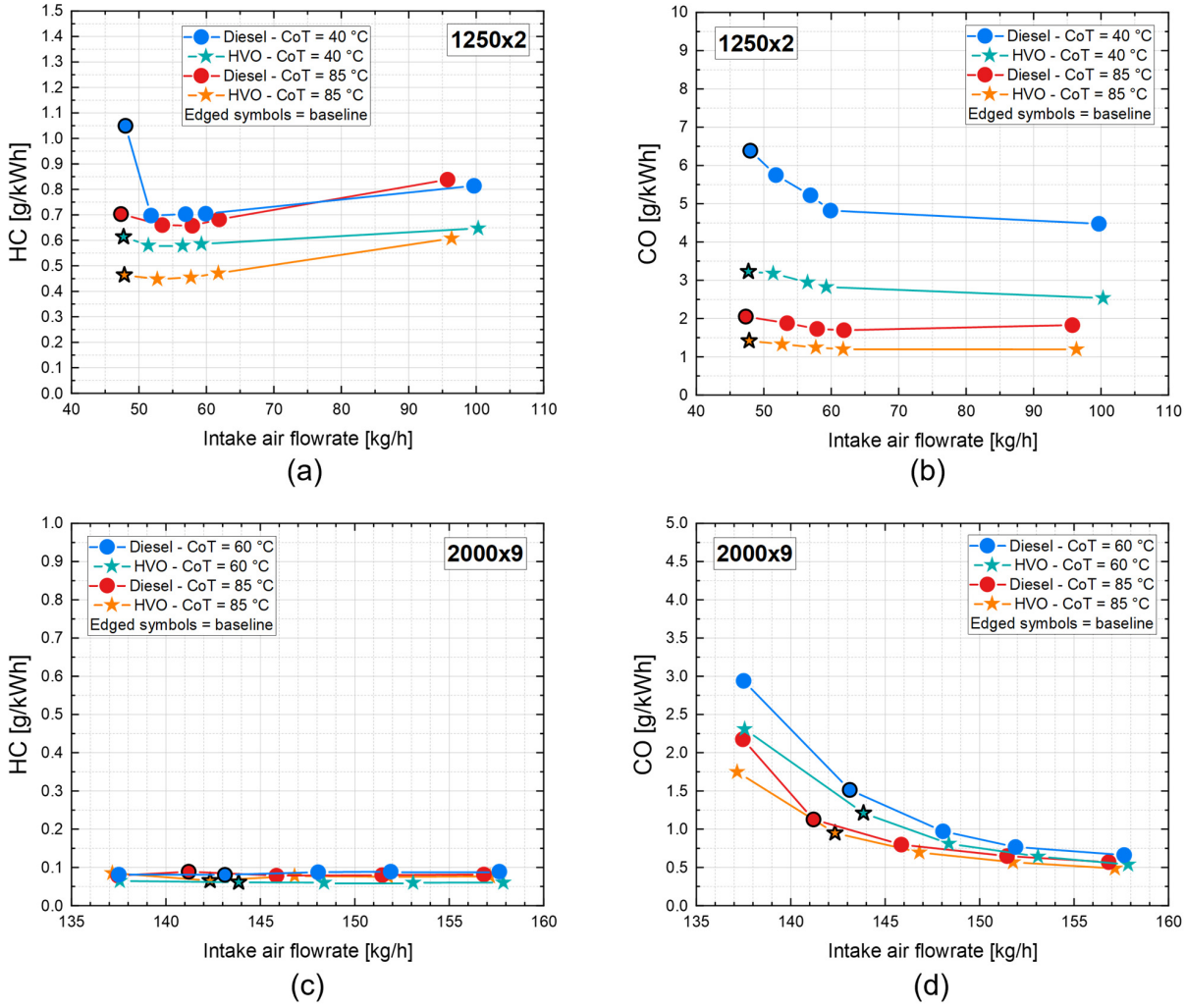

Figure 14. HC and CO emissions along intake air quantity sweep tests at 1250 × 2 (**a**,**b**) and 2000 × 9 (**c**,**d**). Comparison between diesel and HVO at high and low coolant temperatures. Warm colors represent high coolant temperatures, while cool colors represent low coolant temperatures. Circles represent diesel, while stars represent HVO.

At 2000 × 9 CO emissions exhibit roughly the same trend as they do at lower loads, whereas HC emissions are negligible throughout the trade-off.

Engine-Out NO_x and Soot Emissions

As depicted in Figure 15, increasing q_{air} for both fuels results in a decrease in soot levels. This drop is less substantial at lower loads (although HVO still performs better than

diesel) but significant at greater loads. Conversely, NO_x emissions massively decrease by increasing EGR rate (which are very similar between both fuels), at each coolant temperature. At 2000 × 9 and high coolant temperature, however, as depicted in Figure 15d, HVO produces less NO_x at constant intake air. Figure 16a displays EGR rate as a function of intake air flow rate (at 2000 × 9) to explain this. Although boost pressure and $\dot{m}_{air}$ are both kept constant (and fuel-independent), HVO tests feature consistently more EGR, due to the different engine volumetric efficiency and intake temperature (as already explained in previous subsections). It is this difference in EGR that causes NOx variation, rather than specific fuel properties, as confirmed by Figure 16b, which plots NO_x emissions as a function of EGR and shows how all the NO_x-EGR rate trade-offs roughly overlap.

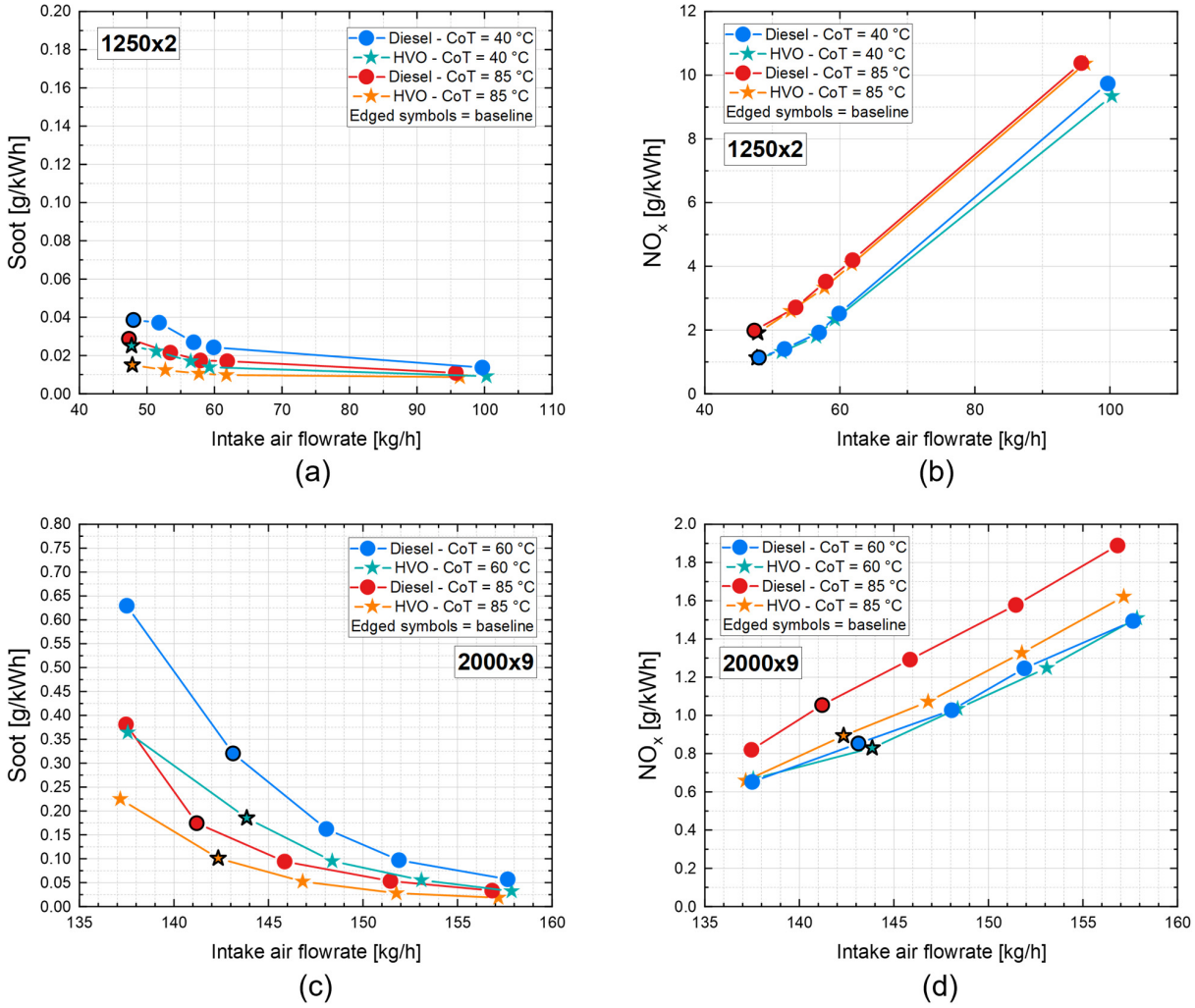

Figure 15. Soot and NOx emissions along intake air quantity sweep tests at 1250 × 2 (**a**,**b**) and 2000 × 9 (**c**,**d**). Comparison between diesel and HVO at high and low coolant temperatures. Warm colors represent high coolant temperatures, while cool colors represent low coolant temperatures. Circles represent diesel, while stars represent HVO.

In general, HVO proves to be more tolerant of EGR than diesel at both low and high coolant temperatures, meaning that HVO trends (of CO, HC, and soot) are generally flatter than diesel and do not show sharp increases at the highest EGR rates. Therefore, since engine-out soot, CO, and HC emissions are consistently lower for HVO, whereas NO_x emissions depend primarily on the EGR rate, NO_x/HC and NO_x/CO trade-offs (which are of primary concern for lower loads) and NO_x/soot trade-off (more significant at higher loads) can be optimized by increasing EGR rate with HVO.

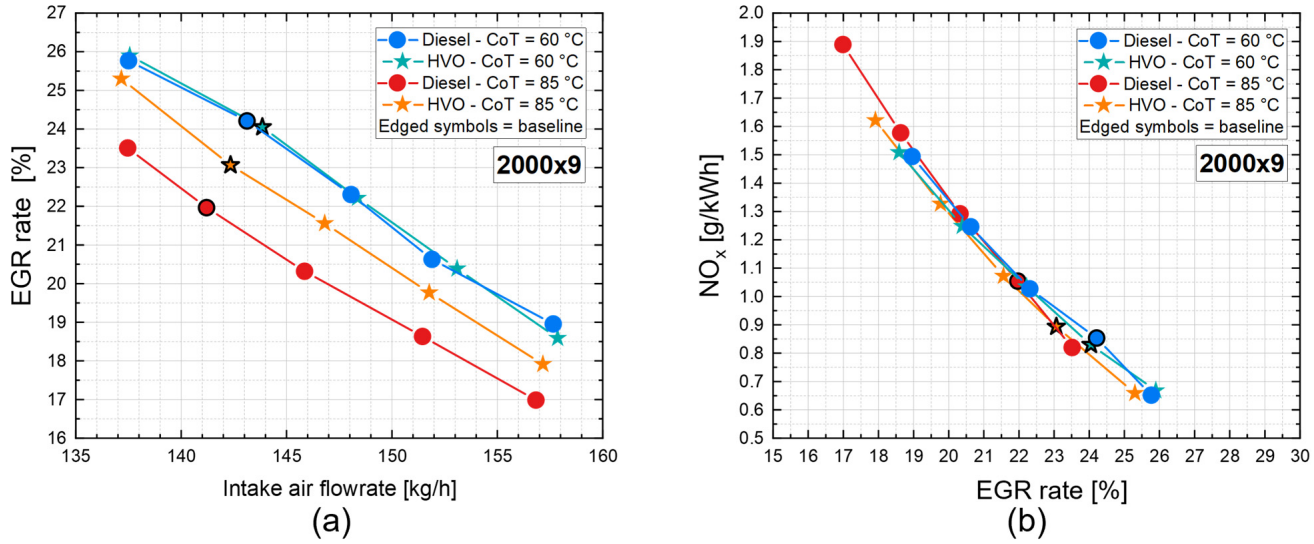

Figure 16. EGR rate as a function of intake air mass flow rate (**a**). The differences between diesel and HVO at high temperature are mainly due to different volumetric efficiency and intake manifold temperature of the engine. NO_x/EGR rate trade-off (**b**).

Engine Thermal Efficiency and Fuel Consumption

At both tested operating points, engine efficiency appears to be comparable between the fuels, as shown in Figure 17. At low load, efficiency trends first increase and then decrease as intake air flow rate rises. The first increment might be due to less EGR, which makes, in general, combustion develop faster and more efficient, while the following decrease might be linked to a stark reduction in intake temperature (due to lower and lower EGR flow rate, till EGR valve progressively closes) that overcomes the effect of efficiency increase due to lower EGR only. However, at high load, efficiency trends are monotonically increasing as intake air flow rate rises.

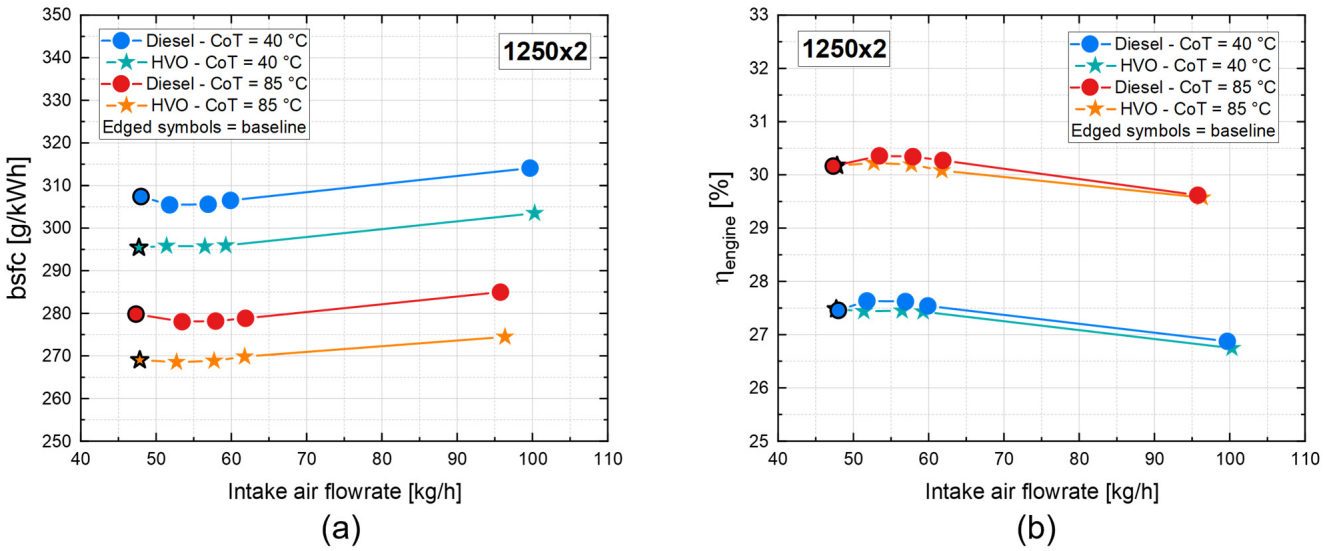

Figure 17. *Cont.*

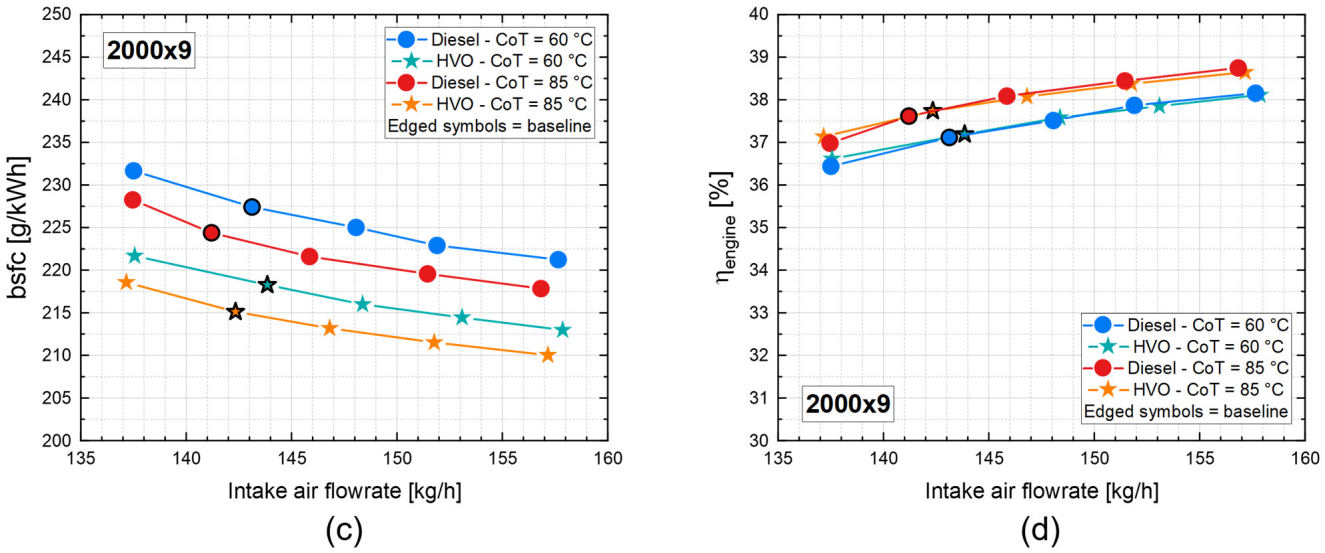

Figure 17. *bsfc* and engine efficiency along intake air quantity sweep tests at 1250 × 2 (**a**,**b**) and 2000 × 9 (**c**,**d**). Comparison between diesel and HVO at high and low coolant temperatures. Warm colors represent high coolant temperatures, while cool colors represent low coolant temperatures. Circles represent diesel, while stars represent HVO.

4. Conclusions

The performance of a diesel engine running on either conventional diesel or HVO at different engine coolant temperatures was examined in this paper. In the first part of the experimental campaign, warm-up/cool-down ramps were performed on two engine operating points. Upon overnight soaking at room temperature, the engine was "naturally" warmed up until the coolant temperature reached 85 °C. Then, by "artificially" adjusting the heat transfer on the coolant side, the coolant water temperature was decreased. A hysteresis pattern on the engine thermal state was highlighted in terms of overall engine behavior and exhaust emissions, whether the engine was just started and "naturally" warmed up or "artificially" cooled down and stabilized at low coolant temperatures.

Next, sweep tests were carried out (on the same engine operating points as the ramp tests) in which the engine was maintained at either high or low coolant temperatures while several engine calibration parameters (SOI_{Main}, p_{Rail} and q_{air}) were varied one-factor at a time, in order to highlight their individual effect on exhaust emissions and engine performance.

In general, it can be stated that HVO emits less engine-out CO, HC, and soot under all examined conditions. Benefits over conventional petroleum-derived diesel tend to intensify at low coolant temperatures, with diesel emissions rising more sharply compared to HVO, both during cold starts and at "artificially" decreased coolant temperature conditions. Furthermore, at both high and low coolant temperatures, HVO appears to be generally more tolerant of variations in engine calibration parameters compared to diesel. HVO emission trends tend to be flatter than diesel, which exhibit sharper deterioration at lower or higher ends of calibration ranges (e.g., lowest p_{Rail}, most delayed SOI_{Main} or highest EGR rate).

NO_x emissions were found to be comparable for both fuels (regardless of coolant temperature and specific ECU calibration). Possibly, small differences can be attributed to small variations in EGR rate. In terms of engine thermal efficiency, too, it appears that the two fuels perform similarly in the majority of the tested conditions. Nevertheless, HVO seems to give non-negligible (up to 2%) improvements in thermal efficiency during cold start and low engine loads, compared to diesel. This may be due to better flammability and cetane number of HVO, which results in a more stable combustion, especially under those conditions.

In conclusion, since HVO tends to produce lower engine-out CO, HC, and soot emissions, especially at low coolant temperatures, exhibiting greater tolerance of calibration parameter changes compared to diesel, the engine calibration work has more room for

maneuver and could exploit generally higher EGR rates, delayed injection timings and/or lower fuel injection pressures to optimize NO_x/thermal efficiency trade-offs.

Author Contributions: Conceptualization, A.M. and O.M.; Methodology, A.M. and O.M.; Software, A.M. and O.M.; Validation, A.M. and O.M.; Formal analysis, A.M. and O.M.; Investigation, A.M. and O.M.; Data curation, A.M. and O.M.; Writing—original draft, A.M. and O.M.; Writing—review & editing, A.M. and O.M.; Visualization, A.M. and O.M. All authors have read and agreed to the published version of the manuscript.

Funding: This research received no external funding.

Data Availability Statement: Data is contained within the article.

Acknowledgments: The Authors would like to acknowledge AVL for the utilization of CAMEO 4.4 and CONCERTO 5.6 within the University Partnership Program.

Conflicts of Interest: The authors declare no conflict of interest.

Abbreviations

ATS	After treatment system
bmeps	Brake mean effective pressure
bsfc	Brake specific fuel consumption
°CA	Crank angle degree
°CA aTDC	Crank angle degree after top dead center
°CA bTDC	Crank angle degree before top dead center
CI	Compression ignition
CoT	Coolant outlet temperature
DOC	Diesel oxidation catalyst
DPF	Diesel particulate filter
ECU	Electronic control unit
EGR	Exhaust gas recirculation
FAME	Fatty acid methyl esters
GHG	Greenhouse gas
HC	Unburned hydrocarbon
HP EGR	High pressure EGR
HVO	Hydrotreated Vegetable Oil
ID	Ignition delay
LP EGR	Low pressure EGR
$\dot{m}_{air}$	Air mass flow rate
MFB50	Crank angle at 50% Mass Fraction Burned
mg/str	milligram per stroke
NO_x	Nitrogen oxides
PID	Proportional, Integrative, Derivative
PM	Particulate matter
p_{Rail}	Rail fuel pressure
q_{air}	Intake air quantity
SCR	Selective reduction catalyst
SOC	Start of combustion
SOI_{Main}	Crank angle at which main injection star
VGT	Variable geometry turbine
η_{engine}	Engine thermal efficiency

References

1. Guo, Y.; Kelly, J.A.; Clinch, J.P. Road Transport Electrification—Is Timing Everything? Implications of Emissions Analysis' Outcomes for Climate and Air Policy. *Transp. Res. Interdiscip. Perspect.* **2021**, *12*, 100478. [CrossRef]
2. Kalghatgi, G. Is It Really the End of Internal Combustion Engines and Petroleum in Transport? *Appl. Energy* **2018**, *225*, 965–974. [CrossRef]
3. Savickas, D.; Steponavičius, D.; Špokas, L.; Saldukaitė, L.; Semenišin, M. Impact of Combine Harvester Technological Operations on Global Warming Potential. *Appl. Sci.* **2021**, *11*, 8662. [CrossRef]

4. Rimkus, A.; Žaglinskis, J.; Stravinskas, S.; Rapalis, P.; Matijošius, J.; Bereczky, Á. Research on the Combustion, Energy and Emission Parameters of Various Concentration Blends of Hydrotreated Vegetable Oil Biofuel and Diesel Fuel in a Compression-Ignition Engine. *Energies* **2019**, *12*, 2978. [CrossRef]
5. Puricelli, S.; Cardellini, G.; Casadei, S.; Faedo, D.; van den Oever, A.E.M.; Grosso, M. A Review on Biofuels for Light-Duty Vehicles in Europe. *Renew. Sustain. Energy Rev.* **2021**, *137*, 110398. [CrossRef]
6. Haines, A.; McMichael, A.J.; Smith, K.R.; Roberts, I.; Woodcock, J.; Markandya, A.; Armstrong, B.G.; Campbell-Lendrum, D.; Dangour, A.D.; Davies, M.; et al. Public Health Benefits of Strategies to Reduce Greenhouse-Gas Emissions: Overview and Implications for Policy Makers. *Lancet* **2009**, *374*, 2104–2114. [CrossRef]
7. European Commission. Transport Emissions, Climate Action. Available online: https://ec.europa.eu/clima/policies/transport_en (accessed on 30 November 2022).
8. Heywood, J.B. *Internal Combustion Engine Fundamentals*; McGraw-Hill Education: New York, NY, USA, 2018.
9. Zeldovich, Y.B. 26. Oxidation of Nitrogen in Combustion and Explosions. In *Selected Works of Yakov Borisovich Zeldovich*; Princeton University Press: Princeton, NJ, USA, 2015; Volume I.
10. Hiroyasu, H.; Arai, M.; Nakanishi, K. Soot Formation and Oxidation in Diesel Engines. In Proceedings of the 1980 Automotive Engineering Congress and Exposition, Detroit, MI, USA, 25 February 1980; SAE International: Warrendale, PA, USA, 1980.
11. Malmborg, V.B.; Eriksson, A.C.; Shen, M.; Nilsson, P.; Gallo, Y.; Waldheim, B.; Martinsson, J.; Andersson, Ö.; Pagels, J. Evolution of In-Cylinder Diesel Engine Soot and Emission Characteristics Investigated with Online Aerosol Mass Spectrometry. *Environ. Sci. Technol.* **2017**, *51*, 1876–1885. [CrossRef]
12. d'Ambrosio, S.; Mancarella, A.; Manelli, A.; Mittica, A.; Hardy, G. Experimental Analysis on the Effects of Multiple Injection Strategies on Pollutant Emissions, Combustion Noise, and Fuel Consumption in a Premixed Charge Compression Ignition Engine. *SAE Int. J. Engines* **2021**, *14*, 611. [CrossRef]
13. D'Ambrosio, S.; Ferrari, A.; Mancarella, A.; Mancò, S.; Mittica, A. Comparison of the Emissions, Noise, and Fuel Consumption Comparison of Direct and Indirect Piezoelectric and Solenoid Injectors in a Low-Compression-Ratio Diesel Engine. *Energies* **2019**, *12*, 4023. [CrossRef]
14. Reşitoğlu, I.A.; Altinişik, K.; Keskin, A. The Pollutant Emissions from Diesel-Engine Vehicles and Exhaust Aftertreatment Systems. *Clean Technol. Environ. Policy* **2015**, *17*, 15–27. [CrossRef]
15. Cococcetta, F.; Finesso, R.; Hardy, G.; Marello, O.; Spessa, E. Implementation and Assessment of a Model-Based Controller of Torque and Nitrogen Oxide Emissions in an 11 L Heavy-Duty Diesel Engine. *Energies* **2019**, *12*, 4704. [CrossRef]
16. d'Ambrosio, S.; Finesso, R.; Hardy, G.; Manelli, A.; Mancarella, A.; Marello, O.; Mittica, A. Model-Based Control of Torque and Nitrogen Oxide Emissions in a Euro VI 3.0 L Diesel Engine through Rapid Prototyping. *Energies* **2021**, *14*, 1107. [CrossRef]
17. Malan, S.A.; Ventura, L.; Manelli, A. Cycle to Cycle Closed-Loop Combustion Control through Virtual Sensor in a Diesel Engine. In Proceedings of the 2021 29th Mediterranean Conference on Control and Automation (MED 2021), Puglia, Italy, 22–25 June 2021.
18. Luo, X.; Wang, S.; de Jager, B.; Willems, P. Cylinder Pressure-Based Combustion Control with Multi-Pulse Fuel Injection. *IFAC-PappersOnLine* **2015**, *28*, 181–186. [CrossRef]
19. Yin, L.; Turesson, G.; Tunestal, P.; Johansson, R. Model Predictive Control of an Advanced Multiple Cylinder Engine with Partially Premixed Combustion Concept. *IEEE/ASME Trans. Mechatron.* **2020**, *25*, 804–814. [CrossRef]
20. Parravicini, M.; Barro, C.; Boulouchos, K. Experimental Characterization of GTL, HVO, and OME Based Alternative Fuels for Diesel Engines. *Fuel* **2021**, *292*, 120177. [CrossRef]
21. Knothe, G. Biodiesel and Renewable Diesel: A Comparison. *Prog. Energy Combust. Sci.* **2010**, *36*, 364–373. [CrossRef]
22. Bortel, I.; Vávra, J.; Takáts, M. Effect of HVO Fuel Mixtures on Emissions and Performance of a Passenger Car Size Diesel Engine. *Renew. Energy* **2019**, *140*, 680–691. [CrossRef]
23. Krivopolianskii, V.; Bjørgen, K.O.P.; Emberson, D.; Ushakov, S.; Æsøy, V.; Løvås, T. Experimental Study of Ignition Delay, Combustion, and NO Emission Characteristics of Hydrogenated Vegetable Oil. *SAE Int. J. Fuels Lubr.* **2019**, *12*, 29–42. [CrossRef]
24. Ohshio, N.; Saito, K.; Kobayashi, S.; Tanaka, S. Storage Stability of FAME Blended Diesel Fuels. In Proceedings of the Powertrains, Fuels and Lubricants Meeting, Chicago, IL, USA, 6–9 October 2008. SAE Technical Papers.
25. Wei, X.F.; Meng, Q.; Kallio, K.J.; Olsson, R.T.; Hedenqvist, M.S. Ageing Properties of a Polyoxymethylene Copolymer Exposed to (Bio) Diesel and Hydrogenated Vegetable Oil (HVO) in Demanding High Temperature Conditions. *Polym. Degrad. Stab.* **2021**, *185*, 109491. [CrossRef]
26. Athanasios, D.; Athanasios, D.; Stylianos, D.; Stella, B.; Samaras, Z. Emissions Optimization Potential of a Diesel Engine Running on HVO: A Combined Experimental and Simulation Investigation. In Proceedings of the 14th International Conference on Engines & Vehicles, Capri, Italy, 10–19 September 2019. SAE Technical Papers.
27. Hartikka, T.; Kuronen, M.; Kiiski, U. Technical Performance of HVO (Hydrotreated Vegetable Oil) in Diesel Engines. In Proceedings of the SAE 2012 International Powertrains, Fuels & Lubricants Meeting, Heidelberg, Germany, 17–19 September 2012; SAE Technical Papers. Volume 9.
28. Mittelbach, M. Fuels from Oils and Fats: Recent Developments and Perspectives. *Eur. J. Lipid Sci. Technol.* **2015**, *117*, 1832–1846. [CrossRef]
29. Suarez-Bertoa, R.; Kousoulidou, M.; Clairotte, M.; Giechaskiel, B.; Nuottimäki, J.; Sarjovaara, T.; Lonza, L. Impact of HVO Blends on Modern Diesel Passenger Cars Emissions during Real World Operation. *Fuel* **2019**, *235*, 1427–1435. [CrossRef]
30. Dimitriadis, A.; Natsios, I.; Dimaratos, A.; Katsaounis, D.; Samaras, Z.; Bezergianni, S.; Lehto, K. Evaluation of a Hydrotreated Vegetable Oil (HVO) and Effects on Emissions of a Passenger Car Diesel Engine. *Front. Mech. Eng.* **2018**, *4*, 7. [CrossRef]

31. Stumborg, M.; Wong, A.; Hogan, E. Hydroprocessed Vegetable Oils for Diesel Fuel Improvement. *Bioresour. Technol.* **1996**, *56*, 13–18. [CrossRef]
32. Zeman, P.; Hönig, V.; Kotek, M.; Táborský, J.; Obergruber, M.; Mařík, J.; Hartová, V.; Pechout, M. Hydrotreated Vegetable Oil as a Fuel from Waste Materials. *Catalysts* **2019**, *9*, 337. [CrossRef]
33. No, S.Y. Application of Hydrotreated Vegetable Oil from Triglyceride Based Biomass to CI Engines—A Review. *Fuel* **2014**, *115*, 88–96. [CrossRef]
34. Bohl, T.; Smallbone, A.; Tian, G.; Roskilly, A.P. Particulate Number and NOx Trade-off Comparisons between HVO and Mineral Diesel in HD Applications. *Fuel* **2018**, *215*, 90–101. [CrossRef]
35. Dobrzyńska, E.; Szewczyńska, M.; Pośniak, M.; Szczotka, A.; Puchałka, B.; Woodburn, J. Exhaust Emissions from Diesel Engines Fueled by Different Blends with the Addition of Nanomodifiers and Hydrotreated Vegetable Oil HVO. *Environ. Pollut.* **2020**, *259*, 113772. [CrossRef]
36. Pflaum, H.; Hofmann, P.; Geringer, B.; Weissel, W. Potential of Hydrogenated Vegetable Oil (HVO) in a Modern Diesel Engine. In Proceedings of the Small Engine Technology Conference & Exposition, Niigata, Japan, 30 October 2010. SAE Technical Papers.
37. d'Ambrosio, S.; Ferrari, A.; Mancarella, A.; Mittica, A. Effects of Rate-Shaped and Multiple Injection Strategies on Pollutant Emissions, Combustion Noise and Fuel Consumption in a Low Compression Ratio Diesel Engine. *Int. J. Automot. Technol.* **2020**, *21*, 197–214. [CrossRef]
38. Botero, M.L.; Mosbach, S.; Kraft, M. Sooting Tendency of Paraffin Components of Diesel and Gasoline in Diffusion Flames. *Fuel* **2014**, *126*, 8–15. [CrossRef]
39. Sugiyama, K.; Goto, I.; Kitano, K.; Mogi, K.; Honkanen, M. Effects of Hydrotreated Vegetable Oil (HVO) as Renewable Diesel Fuel on Combustion and Exhaust Emissions in Diesel Engine. *SAE Int. J. Fuels Lubr.* **2012**, *5*, 205–217. [CrossRef]
40. d'Ambrosio, S.; Mancarella, A.; Manelli, A. Utilization of Hydrotreated Vegetable Oil (HVO) in a Euro 6 Dual-Loop EGR Diesel Engine: Behavior as a Drop-In Fuel and Potentialities along Calibration Parameter Sweeps. *Energies* **2022**, *15*, 7202. [CrossRef]
41. Lodi, F.; Zare, A.; Arora, P.; Stevanovic, S.; Jafari, M.; Ristovski, Z.; Brown, R.J.; Bodisco, T. Combustion Analysis of a Diesel Engine during Warm up at Different Coolant and Lubricating Oil Temperatures. *Energies* **2020**, *13*, 3931. [CrossRef]
42. Weiss, M.; Paffumi, E.; Clairotte, M.; Drossinos, Y.; Vlachos, T. *Including Cold-Start Emissions in the Real-Driving Emissions (RDE) Test Procedure Effects*; Joint Research Centre (JRC): Ispra, Italy, 2017.
43. D'Ambrosio, S.; Finesso, R.; Spessa, E. Calculation of Mass Emissions, Oxygen Mass Fraction and Thermal Capacity of the Inducted Charge in SI and Diesel Engines from Exhaust and Intake Gas Analysis. *Fuel* **2011**, *90*, 152–166. [CrossRef]
44. Jaroonjitsathian, S.; Saisirirat, P.; Sivara, K.; Tongroon, M.; Chollacoop, N. Effects of GTL and HVO Blended Fuels on Combustion and Exhaust Emissions of a Common-Rail Di Diesel Technology. In Proceedings of the SAE 2014 International Powertrain, Fuels & Lubricants Meeting, Birmingham, UK, 20–22 October 2014. SAE Technical Papers.
45. Ventura, L.; Finesso, R.; Malan, S.A.; D'Ambrosio, S.; Manelli, A. Model-Based Design of Closed Loop Controllers of the Air-Path in a Heavy Duty Diesel Engine. In *AIP Conference Proceedings*; AIP Publishing LLC: Melville, NY, USA, 2019; Volume 2191, p. 020152.
46. Finesso, R.; Hardy, G.; Maino, C.; Marello, O.; Spessa, E. A New Control-Oriented Semi-Empirical Approach to Predict Engine-out NOx Emissions in a Euro VI 3.0 L Diesel Engine. *Energies* **2017**, *10*, 1978. [CrossRef]
47. Singh, D.; Subramanian, K.A.; Garg, M.O. Comprehensive Review of Combustion, Performance and Emissions Characteristics of a Compression Ignition Engine Fueled with Hydroprocessed Renewable Diesel. *Renew. Sustain. Energy Rev.* **2018**, *81*, 2947–2954. [CrossRef]
48. Tauzia, X.; Maiboom, A.; Karaky, H.; Chesse, P. Experimental Analysis of the Influence of Coolant and Oil Temperature on Combustion and Emissions in an Automotive Diesel Engine. *Int. J. Engine Res.* **2019**, *20*, 247–260. [CrossRef]
49. Opat, R.; Ra, Y.; Gonzalez D, M.A.; Krieger, R.; Reitz, R.D.; Foster, D.E.; Durrett, R.P.; Siewert, R.M. Investigation of Mixing and Temperature Effects on HC/CO Emissions for Highly Dilute Low Temperature Combustion in a Light Duty Diesel Engine. In Proceedings of the SAE World Congress & Exhibition, Detroit, MI, USA, 16–19 April 2007. SAE Technical Papers.